

# 1 **Comprehensive Automobile Research System (CARS) – a**

## 2 **Python-based Automobile Emissions Inventory Model**

3 Bok H. Baek<sup>1</sup>, Rizzieri Pedruzzi<sup>2</sup>, Minwoo Park<sup>3</sup>, Chi-Tsan Wang<sup>1</sup>, Younha Kim<sup>4</sup>, Chul-Han  
4 Song<sup>5</sup>, and Jung-Hun Woo<sup>3,6</sup>

5 <sup>1</sup>Center for Spatial Information Science and Systems – George Mason University, Fairfax, VA, USA.

6 <sup>2</sup>Department of Sanitary and Environmental Engineering, Federal University of Minas Gerais, Belo Horizonte,  
7 Brazil.

8 <sup>3</sup>Department of Technology Fusion Engineering, College of Engineering, Konkuk University, Seoul, Republic of  
9 Korea

10 <sup>4</sup>Energy, Climate, and Environment program, International Institute for Applied Systems Analysis, Laxenburg,  
11 Austria

12 <sup>5</sup>School of Earth and Environmental Engineering, Gwangju Institute Science and Technology, Gwangju, Republic of  
13 Korea

14 <sup>6</sup>Civil and Environmental Engineering, College of Engineering, Konkuk University, Seoul, Republic of Korea

15 *corresponding to: Jung-Hun Woo (jwoo@konkuk.ac.kr)*

16

### 17 **Abstract**

18 The Comprehensive Automobile Research System (CARS) is an open-source python-based  
19 automobile emissions inventory model designed to efficiently estimate high quality emissions  
20 from motor-vehicle emission sources. It can estimate the criteria air pollutants, greenhouse gases,  
21 and air toxins in any spatial resolution based on the spatiotemporal resolutions of input datasets.

22 The CARS is designed to utilize local vehicle activity data, such as vehicle travel distance, road  
23 link-level network Geographic Information System (GIS) information, and vehicle-specific  
24 average speed by road type, to generate an automobile emissions inventory for policymakers,  
25 stakeholders, and the air quality modeling community. The CARS model adopted the European  
26 Environment Agency's (EEA) onroad automobile emissions calculation methodologies to estimate  
27 the hot exhaust, cold start, and evaporative emissions from onroad automobile sources. It can  
28 optionally utilize average speed distribution (ASD) of all road types to reflect more realistic  
29 vehicle speed variations. Also, through utilizing high-resolution road GIS data, the CARS can  
30 estimate the road link-level emissions to improve the inventory's spatial resolution. When we  
31 compared the official 2015 national mobile emissions from Korea's Clean Air Policy Support  
32 System (CAPSS) against the ones estimated by the CARS, there is a significant increase in volatile

33 organic compounds (VOCs) (33%) and carbon monoxide (CO) (52%) measured, with a slight  
34 increase in fine particulate matter (PM<sub>2.5</sub>) (15%) emissions. Nitrogen oxides (NO<sub>x</sub>) and sulfur  
35 oxides (SO<sub>x</sub>) measurements are reduced by 24% and 17% respectively in the CARS estimates.  
36 The main differences are driven by different vehicle activities and the incorporation of road-  
37 specific ASD, which plays a critical role in hot exhaust emission estimates but wasn't implemented  
38 in Korea's CAPSS mobile emissions inventory. While 52% of vehicles use gasoline fuel and 35%  
39 use diesel, gasoline vehicles only contribute 7.7% of total NO<sub>x</sub> emissions while diesel vehicles  
40 contribute 85.3%. But for VOC emissions, gasoline vehicles contribute 52.1% while diesel  
41 vehicles are limited to 23%. Diesel buses comprise of only 0.3% of vehicles and has the largest  
42 contribution to NO<sub>x</sub> emissions (8.51% of NO<sub>x</sub> total) per vehicle due to having longest daily vehicle  
43 kilometer travel (VKT). For VOC emissions, Compressed Natural Gas (CNG) buses are the largest  
44 contributor at 19.5% of total VOC emissions. For primary PM<sub>2.5</sub>, more than 98.5% is from diesel  
45 vehicles. The CARS model's in-depth analysis feature can assist government policymakers and  
46 stakeholders in developing the best emission abatement strategies.

47 Keywords: inventory: automobile, vehicle emissions, hot exhaust, cold start, evaporative, python

## 48 **1 Introduction**

49 Globally, ambient pollution causes more than 4.2 million premature deaths every year  
50 (Cohen et al., 2017), and Burnett et al. (2018) estimated the health burden is closer to 9 million  
51 deaths from ambient PM concentrations. To effectively mitigate air pollutants, governments have  
52 been implementing stringent air pollution control policies to reduce harmful regional air pollutants  
53 (Hogrefe et al., 2001a; Hogrefe et al., 2001b; Dennis et al., 2010; Rao et al., 2011; Appel et al.,  
54 2013; Luo et al., 2019). The chemical transport model (CTM) simulation results strongly rely on  
55 precise input data, such as emission inventory, meteorology, land surface parameters, and chemical  
56 mechanisms in the atmosphere.

57 The transportation sector is one of the major anthropogenic emissions in urban areas. The  
58 tailpipe emissions from the vehicle's combustion process contain many air pollutants, including  
59 nitrogen oxides (NO<sub>x</sub>), volatile organic compounds (VOCs), carbon monoxide (CO), ammonia  
60 (NH<sub>3</sub>), sulfur dioxide (SO<sub>2</sub>), and primary particulate matter (PM) which participates in the  
61 formation of detrimental secondary pollutants like ozone and PM<sub>2.5</sub> in the atmosphere. In the Seoul  
62 Metropolitan Area (SMA) in South Korea, transportation automobile sources contribute the most  
63 to the total NO<sub>x</sub> and primary PM<sub>2.5</sub> emissions across all emission sources (Choi et al., 2014; Kim  
64 et al., 2017a; Kim et al., 2017b; Kim et al., 2017c). Thus, it is critical to understand and better  
65 represent the emission patterns from transportation automobile sources in the CTM model. The  
66 use of process-based automobile emission models is highly recommended to meet the needs in

67 CTM model because it can estimate high resolution spatiotemporal automobile emissions  
68 (Moussiopoulos et al., 2009; Russell and Dennis, 2000).

69 There are two methodologies known in emission inventory development: top-down and  
70 bottom-up. The choice of methods is determined by the input data availability. The top-down  
71 approach primarily relies on the aggregated and generalized country or regional information, and  
72 is typically used in developing countries where only limited datasets and information are available.  
73 It has its limitations on representing the vehicle emission process realistically due to the lack of  
74 detailed activity and ancillary supporting data. However, the bottom-up approach requires higher  
75 quality spatiotemporal activity datasets like road network information, vehicle composition  
76 (vehicle type, engine size, vehicle age, and fuel-technology), pollutant-specific emissions factors,  
77 road segment length, traffic activity data, and fuel consumption (EEA, 2019; Ibarra-Espinosa et  
78 al., 2018b; IEMA, 2017). It can generate more accurate and detailed automobile emissions across  
79 various operating processes, such as hot exhaust, evaporative, idling, and hot soak (Nagpure et al.,  
80 2016; Ibarra-Espinosa et al., 2018a).

81 There are several bottom-up mobile emissions models available, like MOVES (MOtor  
82 Vehicle Emissions Simulator) from the U.S. Environmental Protection Agency (USEPA), the  
83 European Environment Agency's (EEA) model COPERT (COmputer Programmed to calculate  
84 Emissions from Road Transport), the HERMES (High-Elective Resolution Modelling Emission  
85 System) from Barcelona Supercomputing Center (Guevara et al., 2019), the VEIN (Vehicular  
86 Emissions INventory) model developed by Ibarra-Espinosa et al. (2017), and the VAPI (Vehicular  
87 Air Pollution Inventory) model developed by Nagpure and Gurjar (2012) for India (Nagpure et al.,  
88 2016). While these models are all bottom-up emission inventory models, a single model cannot  
89 meet all modelers, policymakers, and stakeholders' needs because each model holds its own pros  
90 and cons. They are developed differently to meet specific user needs based on the types of traffic  
91 activity and emission factors, emission calculation methodologies, and other traffic related inputs  
92 such as average speed distribution and geographical resolution. Each model is developed with  
93 different levels of specificity, underlying data sets, and modeling assumptions.

94 The MOVES model has the ability to generate high quality emissions for up to 16 different  
95 emission processes (i.e., Running Exhaust, Start Exhaust, Evaporative, Refueling, Extended Idling,  
96 Brake, Tire, etc.). It can simulate not only county-level but also road segment level emissions  
97 depending on data availability. It can also reflect local meteorological conditions, such as ambient  
98 temperature and relative humidity, which can significantly impact both pollutants and emissions  
99 processes (Choi et al., 2017; Perugu et al., 2018). One major disadvantage of this model is that it  
100 is difficult to update and apply to countries outside of the U.S. because it has a high degree of  
101 specificity. The COPERT model, widely used in European countries, can model emissions in high  
102 resolution, is fully integrated with the EEA's onroad vehicle emissions factors guidelines, and can  
103 generate a complete quality assurance (QA) and visualization summary (Ntziachristos et al., 2009).  
104 The cons are that it is a proprietary commercial licensed software, limited to EEA guidance, and

105 challenging to modify and update with any key input datasets like the latest emission factors from  
106 non-European countries (Lejri et al., 2018; Rey DR, 2021; Li et al., 2019; Lv et al., 2019; Smit et  
107 al., 2019).

108 The HERMES and VEIN are both recently released bottom-up inventory models. They  
109 have their pros in that they are both open-source models based on open-source computing  
110 languages (Python and R), which provide transparency of the emission calculations with a  
111 considerable amount of data behind them (Ibarra-Espinosa et al., 2018b; Guevara et al., 2019).  
112 Both models are driven by comma-separated value (CSV) formatted input files, making it very  
113 easy for users to modify the input datasets. They are also based on the EEA's emission calculation  
114 method and equipped with a complete QA and visualization tool based on Python and R libraries.  
115 However, it is not an easy task to develop the emission factors, and other required input datasets  
116 for other countries and implement any control strategy plan feature to generate a responsive  
117 reduced emissions inventory.

118 Overall, there are multiple shortcomings in incorporating these bottom-up models into  
119 CTM studies. They require strong programming skills to operate, such as collecting and preparing  
120 the input data to fit the model requirements, configuring the model variables, and changing specific  
121 variables that may be embedded in the code. Another downside is that while the geographical  
122 administration-level (e.g., county level) emissions inventory can be estimated by these models, it  
123 requires a 3<sup>rd</sup> party emissions processor like the SMOKE (Sparse Matrix Operator Kerner  
124 Emissions) modeling system (Baek and Seppanen, 2021) to process and generate spatially and  
125 temporally resolved emissions inputs for CTM. Some detailed information, like link-level hourly  
126 driving patterns, can be lost in the emissions processing steps.

127 There is no single model capable of meeting all the requirements across various spatial and  
128 temporal scales (Pinto et al., 2020). However, transparency, simplicity, and a user-friendly  
129 interface are requirements for those who mainly work in transportation policy and air quality  
130 modeling development (Fallahshorshani et al., 2012; Kaewunruen et al., 2016; Sallis et al., 2016;  
131 Sun et al., 2016; Tominaga and Stathopoulos, 2016). Thus, the ideal motor vehicle emissions  
132 modeling system would be computationally optimized, easy-to-use, and has a user-friendly  
133 interface. Additionally, the model should easily adapt detailed local activity information and the  
134 state-of-art emission factors as inputs to represent them in the highest resolution possible  
135 temporally and spatially.

136 We have developed the Comprehensive Automobile Research System (CARS) to meet these  
137 requirements, especially for the air quality research community, policymakers, and air quality  
138 modelers. The CARS is a stand-alone, fully modularized, computationally optimized, python-  
139 based automobile emission model. The modularization improves the efficiency of processing times  
140 as once district and road link-level annual/monthly/daily total emissions are computed; the rest of  
141 the processes are optional. It can generate chemically speciated, spatially gridded, hourly

142 emissions for CTMs without any 3<sup>rd</sup> party programs to develop the highest quality CTM-ready  
143 emissions inputs. Details on modularization will be discussed later. The CARS model can be easily  
144 adopted and is simple for users to add new functions or modules in the future. The application of  
145 the CARS to South Korea will be described in detail later.

## 146 **2 CARS Emissions Calculation**

147 The CARS is an open-source Python-based customizable motor vehicle emissions  
148 processor that estimates onroad and offroad emissions for specific criteria and toxic air pollutants.  
149 Figure 1 is a schematic of the CARS overview. It applies vehicle, engine, and fuel specific  
150 emission factors to traffic data to estimate the local level annual, monthly, and daily total emissions  
151 inventory. The emissions inventory calculations require a list of pollutant-specific emissions  
152 factors by vehicle age, local activity data, average speed profile/distribution by road type, and  
153 geographic information system (GIS) road segment shapefiles inputs. The spatial resolution of  
154 vehicle kilometer travel (VKT) determines the CARS geographic scale (i.e. district, county, state,  
155 and country) for emission calculations. Unlike the district-level Korea Clean Air Policy Support  
156 System (CAPSS) automobile emission inventory (Lee et al., 2011a; Lee et al., 2011b), the CARS  
157 applies high resolution annual average daily traffic (AADT) data from the road GIS shapefiles to  
158 distribute the total district emissions into road link-level emissions. Optionally, these road link-  
159 level emissions can be used to generate spatially gridded CTM-ready emissions input data once  
160 the output modeling domain is defined. The summary of input files by categories are presented in  
161 Appendix H. How the CARS estimates spatially and temporally enhanced automobile emissions  
162 inventories will be discussed in detail next chapter.

163 South Korean traffic databases from the Korea National Institute of Environmental  
164 Research (NIER) CAPSS team (Lee et al., 2011b) were used in this study to compute the updated  
165 onroad automobile emissions inventory. The databases include individual vehicle activity data  
166 (daily total VKT), road activity data (average speed distribution by road), vehicle age specific  
167 emission factors, road type information, surface weather data, and GIS road shapefiles.

### 168 **2.1 Individual Daily Average VKT Activity Data**

169 The individual vehicle VKT data is used to reflect human activity. This study imported the  
170 national registered vehicle-specific daily total VKT from South Korea's Vehicle Inspection  
171 Management System (VIMS), which belongs to the Korea Transportation Safety Authority  
172 (KTSA). It contains over 50 million records of vehicle-specific daily total VKT from 2013 to 2017.  
173 For the CARS model, we first sorted these records by the vehicle identification number (VIN) to  
174 remove any duplicates and then built vehicle-specific daily total VKT traffic activity data in the  
175 CSV format. The summary of those vehicle numbers and VKTs is presented in Fig. 2. Sedan  
176 vehicles using gasoline fuel comprise the greatest percentage of total vehicles at 47% (~10.4

177 million) and have the highest VKT. While most vehicles demonstrate a paired pattern between the  
178 number of vehicles and daily VKT, LPG (liquefied petroleum gas)-fueled taxi shows high VKT  
179 with low vehicle numbers due to their long distance travel daily patterns.

180 The VIN ( $vin$ ) information is used to calculate vehicle-specific daily average VKT ( $VKT_{vin}$ ,  
181  $\text{km d}^{-1}$ ). In Eq. (1), the individual daily average vehicle VKT ( $VKT_{vin}$ ) is calculated based on the  
182 cumulative mileage ( $M_{f,vin}$ ) between the last inspection date ( $D_{f,vin}$ ) and registration date ( $D_{0,vin}$ ).  
183 Each vehicle is categorized with Korea's NIER based on a combination of vehicle types (e.g.,  
184 sedan, truck, bus, etc), engine sizes (e.g., compact, full size, midsize, etc), and fuel types (e.g.,  
185 gasoline, diesel, LPG, etc). Full details of vehicle types and daily total VKT are shown in Appendix  
186 A and B.

$$187 \quad VKT_{vin} = \frac{M_{f,vin}}{D_{f,vin} - D_{0,vin}} \quad (1)$$

## 188 2.2 Emission Calculations

189 Automobile emission sources include motorized engine sources on the paved road network  
190 and off the road network (e.g., driveway and parking lots). The CARS model doesn't currently  
191 simulate emissions from nonroad emission sources, such as aviation, railways, construction,  
192 agricultures, lawn mowers, and boats. The CARS model simulates the onroad automobile  
193 emissions from network roads using their local traffic-related datasets. The following section  
194 explains the approach of the onroad automobile emission processes. The onroad emission ( $E_{onroad}$ )  
195 in the CARS is defined in Eq. (2), which includes three major emission processes (Ntziachristos  
196 and Samaras, 2000):

$$197 \quad E_{onroad} = E_{hot} + E_{cold} + E_{vap} \quad (2)$$

198 The hot exhaust emissions ( $E_{hot}$ ) are the vehicle's tailpipe emissions when the internal combustion  
199 engine (ICE) combusts the fuel to generate energy under the average operating temperature. The  
200 cold start emissions ( $E_{cold}$ ) are the tailpipe emissions from the ICE when the cold vehicle engine is  
201 ignited and the operational temperature is below average condition. The evaporative VOC  
202 emissions ( $E_{vap}$ ) are the emissions evaporated/permeated from the fuel systems (fuel tanks,  
203 injection systems, and fuel lines) of vehicles.

204 The CARS first applies the hot exhaust emission factors by vehicle type, age, fuel, engine,  
205 and pollutants to individual daily total VKT to compute the hot exhaust emissions. The rest of the  
206 processes for cold start and evaporative emissions are calculated afterwards. The emission  
207 calculation methodologies used in the CARS model are based on tier 2 and tier 3 methodologies  
208 from the EEA's mobile emission inventory guidebook (EEA, 2019) to be consistent with Korea's  
209 National Emission Inventory System (NEIS) (Lee et al., 2011a).

## 2.2.1 Hot Exhaust Emissions

Hot exhaust emissions is the exhaust gas from the combustion process in an ICE. The ICE combustion cycle generally causes incomplete combustion processes which emit hydrocarbons, carbon monoxide (CO), and particulate matter (PM). These are not completely controlled by the after-treatment equipment, such as a three-way catalytic converter, and released into the atmosphere. The sulfur compounds in the fuel are oxidized and become sulfur oxides (SO<sub>x</sub>). Nitrogen oxides (NO<sub>x</sub>) are produced due to the abundance of nitrogen (N<sub>2</sub>) and oxygen (O<sub>2</sub>) during the combustion process.

Equation 3 represents the calculation of daily individual vehicle hot exhaust emission rate,  $E_{hot;p,vin,myr}$  (g d<sup>-1</sup>) of pollutant ( $p$ ). An individual vehicle-specific daily  $VKT_{vin}$  (km d<sup>-1</sup>) is estimated by Eq. (1). The  $EF_{hot;p,v,myr,s}$  (g/km) is the hot exhaust emission factor of pollutants ( $p$ ) for the vehicle type ( $v$ ), vehicle manufacture year ( $myr$ ), and average vehicle speed ( $s$ ). The district's total emission rate is the total hot exhaust emissions from all individual vehicles within the same district.

$$E_{hot;p,vin,myr} = DF_{p,v,myr} \times VKT_{vin} \times EF_{hot;p,v,myr,s} \quad (3)$$

The deterioration factor ( $DF$ ) in Eq. (3) is an optional function in the CARS. The deterioration process is caused by vehicle aging and can lead to the increase of vehicle emissions. The vehicle  $DF$  is varied by vehicle type ( $v$ ), pollutant ( $p$ ), and vehicle manufacture year ( $myr$ ). The CARS model computes vehicle ages based on the vehicle manufacture year and model simulation year. According to NIER's guidance on calculating deterioration factors, there is no deterioration in a new vehicle during their first five years. After five years, the deterioration factors can range from 5% to 10% depending on the type of vehicle and pollutants. Deterioration processes can cause up to an 100% increase of emissions in fifteen-year-old vehicles. Currently, the  $DF$  is an empirical coefficient that varies by vehicle age (Lee et al., 2011a).

The hot exhaust emission factor,  $EF_{hot;p,v,s}$  (g/km) is a function of vehicle speed ( $s$ ) with other empirical coefficients:  $a, b, c, d, f, k$ . The emission factor formula and those coefficients were developed by NIER's CAPSS (Lee et al., 2011a). These coefficients are varied by pollutants ( $p$ ), vehicle type ( $v$ ), vehicle manufacture year ( $myr$ ), and vehicle speed ( $s$ ). The vehicle speed affects the combustion efficiency of an ICE and impacts the emission rates and its composition from the tailpipe.

$$EF_{hot;p,v,myr,s} = k(a \times s^b + c \times s^d + f) \quad (4)$$

While vehicle speed plays a critical role in hot exhaust emissions from most vehicles, NO<sub>x</sub> emissions from some diesel vehicles show sensitivity to local ambient temperature and humidity due to the atmospheric moisture suppression of high combustion temperatures that lower NO<sub>x</sub> emissions at higher humidity (Choi et al., 2017; Ntziachristos and Samaras, 2000). Figure 3 shows

244 the dependency of NO<sub>x</sub> emission factors from compact diesel vehicles to vehicle speed (Fig. 3a)  
245 and ambient temperature (Fig. 3b). Figure 3a shows a significant decrease of NO<sub>x</sub> emissions when  
246 the speed increases between 0 and 70 km. Figure 3b demonstrates the significance of local  
247 meteorology on NO<sub>x</sub> emissions from a compact diesel sedan. Based on these NIER's CAPSS  
248 emission factors, the sensitivity to local ambient temperature is limited to NO<sub>x</sub> pollutant emissions  
249 from diesel vehicles.

250 Due to its high sensitivity to the vehicle operating speed, it is important for the CARS to  
251 simulate realistic speed patterns for accurate emissions estimates. When a single speed is assigned  
252 to compute hot exhaust emissions, it won't reflect the emissions under low-speed circumstances.  
253 To overcome this limitation, the CARS has adopted the 16 average speed bins concepts for a better  
254 representation of vehicle speed distribution that varies by road type (i.e., local, highway,  
255 expressway). We have implemented a feature for the CARS optionally to apply road-specific  
256 average speed distributions (ASD) ( $A_{bin,r}$ ) by 16 speed bins (*bin*) (from 0 to 121 km h<sup>-1</sup> defined in  
257 Appendix E) for eight different road types (*r*) (No.101-108, shown in Appendix C) as classified  
258 by CAPSS (Fig. 4a). Although ASD patterns vary by region and time, the current CARS model  
259 version does not support ASD application by region and time of day due to the lack its availability  
260 in South Korea.

261 We first developed the ASD (Fig. 4a) for eight different road types (No. 101-108) in South  
262 Korea based on the latest road link-specific average speed and the length of link from the SK GIS  
263 road network shapefiles (NIER, 2018). However, the ASD based on the SK GIS road shapefiles  
264 did not capture low speed (<16 km h<sup>-1</sup>) driving (Fig. 4a). This causes a significantly lower  
265 estimation of NO<sub>x</sub> and VOC emissions compared to the CAPSS (Appendix G). We believe the  
266 SK average speed distribution is missing low speed driving that can occur due to traffic congestion.  
267 To address this absence of low-speed driving in the SK ASD, we incorporated data from the ASD  
268 (Figure 4b) from the state of Georgia to the low speed ranges (speed bin #1 and #2 for road type 1  
269 to 7). We increased the total fractions of low speed bins (the 2:1 ratio of fractions of bin #1 and  
270 #2) by 2% for interstate expressways, 3% for urban expressways, 7% for all highways, and 15%  
271 for all local roads. The increases in low speed bins lowered the distributions of other higher speed  
272 bins homogeneously due to the renormalization of fractions by road type. Figure 4c shows the  
273 renormalized hybrid-ASDs of all road types based on SK ASD and Georgia ASD. We understand  
274 that the hybrid-ASD approach is not ideal for SK onroad emission inventory development, but it  
275 clearly demonstrates the CARS's capability and sensitivity to the vehicle speed representation.

276 While 16 speed bins ASD application is critical to computing more realistic hot exhaust  
277 emissions, there should be some restrictions on certain road types. Users can adjust the restricted  
278 roads control table input file to limit the vehicle types that are only operated on a particular road  
279 type. For example, motorcycles are limited to local roads (No. 104, 106, and 107), but not on  
280 expressways (No. 101, 102, 103, 105, and 108) due to its traffic regulation rules. Heavy trucks are  
281 only allowed on the highway (No. 101, 102, 103, 105, and 108.) by law. The details of the road



282 restriction control table format can be found on the CARS's user's guide from the CARS **version**  
 283 **1 used in this paper** (Baek et al., 2021).

284 The 16 speed bins ASD from Eq. (13) are added to the CARS hot exhaust emissions  
 285 equation (Eq. 3). The hot exhaust emissions from individual vehicles ( $E_{hot;p,vin,myr}$ ) can be  
 286 calculated by considering road-specific speed bins distribution (Eq. 5). Although the vehicles may  
 287 be operated in different districts from their registered district, this is our best method to estimate  
 288 the vehicle speed for hot exhaust emissions.

$$289 \quad E_{hot;p,vin,myr} = DF_{p,v,myr} \times \sum_{bin} (VKT_{vin} \times EF_{hot;p,v,myr,s} \times A_{bin,r}) \quad (5)$$

### 290 **2.2.2 Cold Start Emissions**

291 The cold start emissions occur when a cold engine vehicle is ignited. Lower temperatures  
 292 of the ICE are not optimal conditions for complete fuel combustion. This process lowers the  
 293 combustion efficiency (CE) and increases the emissions of hydrocarbon and CO pollutants from  
 294 the tailpipe exhaust (Jang et al., 2007). The CARS can estimate the cold start emissions for vehicles  
 295 using gasoline, diesel, or liquefied petroleum gas (LPG) fuel. Besides the vehicle and engine type,  
 296 road type also plays a critical role in the quantity of cold start emissions because it occurs mostly  
 297 in parking lots and rarely on highways.

298 The cold start emission,  $E_{cold}$  (g d<sup>-1</sup>), is derived from the hot exhaust emissions, the ratio of  
 299 hot to cold exhaust emissions ( $EF_{cold}/EF_{hot} - 1.0$ ), and the percentage of the traveled distance with  
 300 a cold engine (Eq. 6).

$$301 \quad E_{cold;p,v} = \beta_T \times E_{hot;p,v} \times \left( \frac{EF_{cold;p,v}}{EF_{hot;p,v}} - 1.0 \right) \quad (6)$$

302 The emission factor of cold start emissions ( $EF_{cold}$ ) is not directly calculated from  
 303 measurement data like hot exhaust emissions ( $E_{hot;p,v}$ ), but measured under different ambient  
 304 temperatures ( $T$ ). The CARS model applies linear regression models developed by CAPSS to  
 305 estimate the increasing ratio of cold start to hot exhaust emissions ( $EF_{cold}/EF_{hot}$ ) under different  
 306 temperatures ( $T$ ) (Eq. 7). In this equation,  $A$  and  $B$  are the empirical coefficients that vary by the  
 307 pollutants ( $p$ ) and vehicle type ( $v$ ).

$$308 \quad \left( \frac{EF_{cold;p,v}}{EF_{hot;p,v}} \right) = A_{p,v} + B_{p,v} \times T \quad (7)$$

309  $\beta$  is the percentage of the distance traveled under a cold engine and also depends on the  
 310 ambient temperature. Cold ambient temperatures cause a longer distance traveled under a cold  
 311 engine due to the slower heating time. According to the CAPSS database for Seoul city (Lee et al.,  
 312 2011a), the empirical linear equation for  $\beta$  is shown in Eq. (8). This formula represents how

313 ambient temperature affects  $\beta$ . For example, when the average temperature is  $-2^{\circ}\text{C}$ ,  $\beta$  is 34.8%. In  
 314 summer, the monthly average temperature is  $25.7^{\circ}\text{C}$ , which causes  $\beta$  to drop to 21%.

$$315 \quad \beta = 0.647 - 0.025 \times 12.35 - (0.00974 - 0.000385 \times 12.35) \times T \quad (8)$$

### 316 2.2.3 Evaporative VOC Emissions

317 Evaporative emissions are emissions from vehicle fuel that are evaporated into the  
 318 atmosphere. This occurs in the fueling system inside the vehicle, such as fuel-tanks, injection  
 319 systems, and fuel lines. Diesel vehicles, however, can be exempted due to diesel fuel's low vapor  
 320 pressure. The primary sources of evaporative emissions are breathing losses through tank vents  
 321 and fuel permeation/leakage. The CARS model adopted the EEA's emission inventory guidebook  
 322 (EEA, 2019) to account for diurnal emissions from the tank ( $e_d$ ), hot and warm soak emissions by  
 323 fuel injection type ( $S_{fi}$ ), and running loss emissions ( $R$ ) (Eq. 9). Unlike CAPSS, there is a  
 324 conversion factor (0.075) applied to  $E_{vap}$  for motorcycles to prevent an overestimation of VOC.

$$325 \quad E_{vap;p,v} = (e_{d;p,v} + S_{fi;p,v} + R_{l;p,v}) \quad (9)$$

326 Diurnal emissions,  $e_d$  ( $\text{g d}^{-1}$ ), during the daytime are caused by the ambient temperature  
 327 increase and the expansion of fuel vapors inside the fuel tank. Most of the current fuel tank systems  
 328 have emission control systems to limit this kind of evaporative VOC emissions. The  $e_d$  can be  
 329 calculated with the empirical Eq. (10), which was developed by CAPSS.  $T_l$  is the monthly average  
 330 of the daily lowest temperatures and  $T_h$  is the monthly average of the daily highest temperatures.  
 331 The empirical coefficient  $\alpha$  is 0.2, which represents how 80% of emissions are eliminated by the  
 332 vehicle emission control system.

$$333 \quad e_d = \alpha \times 9.1 \exp[0.3286 + 0.0574 \times (T_l) + 0.0614 \times (T_h - T_l - 11.7)] \quad (10)$$

334 Soak emissions ( $S_{fi}$ ) occur when a hot ICE is turned off; the remaining heat from the ICE  
 335 can increase the fuel temperature in the system which causes the increase of evaporative VOC  
 336 emissions. This carburetor float bowls are the major source of the soak emissions. Newer vehicles  
 337 with fuel injection and returnless fuel systems do not emit soak emissions. Because most of the  
 338 current vehicles in South Korea have a new fuel system, soak emissions ( $S_{fi}$ ) in the CARS model  
 339 are set to 0.

340 The running loss emissions ( $R_l$ ) are from vapors generated in the fuel tank when a vehicle  
 341 is in operation (Eq. 11). In some older vehicles, the carburetor and engine operation can increase  
 342 the temperature in the fuel tank and carburetor, which can cause a significant increase in  
 343 evaporative VOC emissions. VOC emissions from running loss can be greatly increased during  
 344 warmer weather. However, newer vehicles with fuel injection and returnless fuel systems are not

345 affected by the ambient temperature. Because most vehicles in South Korea do not use carburetor  
 346 technology, we expect running loss emissions to have the least impact (Lee et al., 2011b).

$$347 \quad R_l = \alpha \times L_{r,v} \times [(1 - \beta) \times R_h + \beta \times R_w] \quad (11)$$

348 The empirical coefficient  $\alpha$  is 0.1 here, which represents that 90% of the running loss is  
 349 avoided by the newer fuel system.  $L$  is the distance traveled (km) by road and is the same one used  
 350 in hot exhaust emission calculations.  $\beta$  is the same parameter from Eq. (8). The  $R_h$  and  $R_w$  are the  
 351 average emission factors from running loss under hot and warm/cold conditions, respectively.

### 352 2.3 Road Link-Level Emissions Calculations

353 In general, district-level automobile emissions calculations are driven by district-level  
 354 averaged vehicle activity and operating data, which do not reflect realistic spatial patterns of  
 355 onroad automobile emissions. The CARS model introduces road link-specific traffic data by  
 356 default to develop spatially enhanced road link-specific emissions that are more representative of  
 357 the emissions. This high-resolution traffic data is a GIS shapefile that is composed of many  
 358 connected segments, which are called “road links.” All road links hold information such as  
 359 start/end location coordinates, AADT, road link length, averaged vehicle speed, and road type (No.  
 360 101-108).

361 The CARS model applies link-level AADT ( $AADT_{d,r,l}$ ,  $d^{-1}$ ) and road length ( $L_{d,r,l}$ ) to  
 362 compute the road link-specific VKT ( $VKT_{d,r,l}$ ,  $km\ d^{-1}$ ) in Eq. (12). The road links are identified by  
 363 district ( $d$ ), road type ( $r$ ), and link ( $l$ ) labels. The road VKT is a parameter that reflects the traffic  
 364 activity of each road link and it is different from individual daily vehicle activity data ( $VKT_{v,age}$ )  
 365 in Eq. (1).

$$366 \quad VKT_{d,r,l} = AADT_{d,r,l} \times L_{d,r,l} \quad (12)$$

367 Road link-specific VKT ( $VKT_{d,r,l}$ ) is used to redistribute the district total emissions ( $E_{onroad}$ )  
 368 from Eq. 2 into road link-level emissions. The following three weight factors are computed: the  
 369 district weight factors,  $\omega_d$  (Eq. 13), the road type weight factors,  $\omega_{d,r}$  (Eq. 14), and the road-link  
 370 weight factors,  $\omega_{d,l}$  (Eq. 15). The weight district factors ( $\omega_d$ ) are the renormalization of each  
 371 district's total VKT over state-level total VKT ( $N$  is the number of districts). The main reason we  
 372 performed the renormalization over state-level total VKT is to reflect daily traffic patterns from  
 373 multiple districts under the assumption that most vehicles travel within the same state. The road  
 374 type weight factors by district ( $\omega_{r,d}$ ) are used to compute road-specific emissions, while road-  
 375 specific averaged speed distributions (ASD;  $A_{s,r}$ ) from Eq. (5) are applied to capture vehicle  
 376 operating speeds by road type. The road link weight factors ( $\omega_{d,l}$ ) are then applied to redistribute  
 377 the district emissions into road link-level emissions.

378

$$379 \quad \omega_d = \frac{\sum_r \sum_l VKT_{d,r,l}}{\frac{1}{N} \sum_d \sum_r \sum_l VKT_{d,r,l}} \quad (13)$$

$$380 \quad \omega_{d,r} = \frac{\sum_l VKT_{d,r,l}}{\sum_r \sum_l VKT_{d,r,l}} \quad (14)$$

$$381 \quad \omega_{d,l} = \frac{VK T_{d,r,l}}{\sum_r \sum_l VK T_{d,r,l}} \quad (15)$$

### 382 **3 CARS Configuration**

383 The CARS model is an open-source program based on Python (Guido van Rossum, 2009)  
384 that allows the users to efficiently apply open-source modules to develop programs. Users can  
385 easily install Python development tools and load customized packages and modules to set up the  
386 CARS development environment. All CARS modules are developed using Python v3.6. Other than  
387 the GIS road shapefiles, all input files are based in the ASCII CSV format, which can be easily  
388 handled by both spreadsheet programs and programming languages, making it more accessible for  
389 users of all skillsets. The CARS can not only estimate district-level and spatially enhanced road  
390 link-level emissions, but can also generate hourly chemically speciated gridded emissions for  
391 CTMs. In addition, the CARS also generates various summary reports, graphics, and  
392 georeferenced plots for quality assurance.

393 The required Python modules for the CARS are: “*geopandas*,” “*shapely.geometry*,” and  
394 “*csv*” modules to read the shapefiles and table data files. The “*NumPy*” and “*pandas*” modules  
395 are used to operate the memory arrays and scientific calculations, while the “*pyproj*” module deals  
396 with converting the projection coordinate systems. “*matplotlib*” is for generating any type of  
397 figures/plots. Furthermore, the CARS model can also read and write Climate and Forecast (CF)-  
398 compliant NetCDF-formatted files using “*NetCDF4*”.

399 The first process in the CARS is “*Loading\_function\_path*”; it allows users to define and  
400 check the input file paths. Once all input files are checked, there are six process modules in CARS  
401 to process inputs, compute emissions, and generate various output files, including QA reports.  
402 Figure 5 is the schematic of the CARS that consists of six process modules with various functions.  
403 The six process modules are (1) “**Process activity data**”, (2) “**Process emission factors**”, (3)  
404 “**Process shapefile**”, (4) “**Calculate district emissions**”, (5) “**Grid4AQM**”, and (6) “**Plot figures**”.  
405 The main purpose of modularizing the CARS is to meet the needs of various communities, such  
406 as policymakers, stakeholders, and air quality modelers. While modules (1) through (4) are  
407 required to develop the district-level and road link-level emissions inventories, module (5)  
408 “**Grid4AQM**” is optional depending on if users want to develop chemically-speciated gridded  
409 hourly emissions for CTMs. Also, the modularity of the CARS allows users to bypass certain

410 modules if it has been previously processed without any changes. For example, if there is no  
411 change in traffic activity, emission factors table, or GIS shapefiles, users do not need to run these  
412 modules and can simply read the data frame outputs and then run “**Grid4AQM**” for the modeling  
413 dates and domain. The “**Grid4AQM**” module will not only improve the computational time for  
414 CTMs but also eliminate the need for a 3<sup>rd</sup> party emissions modeling system like SMOKE (Baek  
415 and Seppanen, 2021).

416 The rectangle boxes in Fig. 5 represent the data array and the boxes with rounded edges are  
417 the functions in the CARS. Details on the CARS code, input table format, and functions setup  
418 information can be found on the CARS GitHub website (Pedruzzi *et al.*, 2020).

419 The “**Process activity data**” module first reads the vehicle activity data, such as an  
420 individual vehicle's daily total VKT based on its registered district. The “**Process emission factors**”  
421 module reads and stores the emission factors table that holds all pollutant emission factors to  
422 estimate the emissions for all vehicles. Meteorology-sensitive emission factors are only limited to  
423 NO<sub>x</sub> pollutants. District boundary GIS shapefiles and road network shapefiles are processed  
424 through “**Process shape file**” to generate the VKT-based redistribution weighting factors from Eq.  
425 (13), (14) and (15) for the “**Calculate district emissions**” module to compute district-level and  
426 road link-level emission rates (metric tons per year, t yr<sup>-1</sup>).

427 The redistributed emission rates (t yr<sup>-1</sup>) from the “**Calculate district emissions**” module  
428 present annual total emission rates until district-level VKTs from the “**Process activity data**”  
429 module are added. Then, the “**Grid4AQM**” module can generate CTM-ready chemically speciated  
430 emissions. The “**Read\_chemical**” function from the “**Grid4AQM**” module is designed to process  
431 the chemical speciation profile that can convert the inventory pollutants such as CO, NO<sub>x</sub>, SO<sub>2</sub>,  
432 PM<sub>10</sub>, PM<sub>2.5</sub>, VOC, and NH<sub>3</sub>, into the chemically lumped model species that CTM requires for  
433 chemical mechanisms, such as SAPRC (L. and Heo, 2012) and Carbon Bond version 6 (CB6)  
434 (Yarwood and Jung, 2010). The “**Read\_temporal**” function processes the complete set of monthly,  
435 weekly, and hourly temporal allocation profiles that can convert annual total emissions to hourly  
436 emissions. “**Read\_griddesc**” defines the CTM-ready modeling domain and computes the gridding  
437 fractions for all road link-level emissions by overlaying the modeling domain over the GIS  
438 shapefiles. Once annual total emissions are chemically speciated, spatially gridded, and temporally  
439 allocated into hourly emissions, the “**Gridded\_emis**” function will combine emission source-level  
440 conversion fractions from each function (**Read\_chemical**, **Read\_temporal**, and **Read\_griddesc**) to  
441 generate the CTM-ready chemically speciated, gridded hourly emissions in the NetCDF binary  
442 format. The “**Plot Figures**” module is designed for generating various summary reports and  
443 graphics to assist users in understanding the estimated automobile emissions inventory computed  
444 by the CARS. The following section will describe the detailed processes of the “**Grid4AQM**”  
445 module, which includes chemical, spatial, and temporal allocations.

446 The influence of temperature on emission processes are considered in the CARS model.  
447 There are three temperature parameters in current CARS model such as “temp\_max” for maximum  
448 temperature, “temp\_mean” for mean temperature, and “temp\_min” for minimum temperature.  
449 These temperature parameters will be applied to over the entire modeling domain during the  
450 simulation period. Current CARS model version does not support to process gridded meteorology  
451 data from the 3<sup>rd</sup> party meteorology models like Meteorology-Chemistry Interface Processor  
452 (MCIP) from U.S. EPA., and Weather Research Forecasting (WRF) model from National Center  
453 for Atmospheric Research (NCAR) yet. However, CARS can easily adopt various temporally  
454 resolved temperature values by adjusting the CARS simulation period (i.e., day, week, month,  
455 season, or annual).

### 456 3.1 Chemical Speciation

457 To support CTMs applications, the CARS needs to be able to convert inventory pollutants  
458 into chemical lumped model species based on the choice of CTM chemical mechanisms. NO<sub>x</sub>  
459 includes nitric oxide (NO), nitrogen dioxide (NO<sub>2</sub>), and nitrous acid (HONO). VOCs can represent  
460 hundreds of different organic carbon species, such as benzene, acetaldehyde, and formaldehyde.  
461 These grouped inventory pollutants cannot be directly imported into the chemical mechanism  
462 modules in the CTM system and require chemical speciation allocation for CTMs to process them  
463 during their chemical reactions. Therefore, the “**Grid4AQM**” module performs the chemical  
464 species allocation step prior to the temporal and spatial allocations to generate the gridded hourly  
465 emissions. The “*Read\_chemical*” function in “**Grid4AQM**” module allows users to assign these  
466 emission inventory pollutants to CTM-ready surrogate chemical species (a.k.a lumped chemical  
467 species) by vehicle, engine, and fuel type. For example, VOC emissions from diesel busses can be  
468 converted into the following composition based on its chemical allocation profile: alkanes (68%),  
469 toluene (9%), xylenes (8%), alkenes (4%), ethylene (2%), benzene (1.3%), and unreactive  
470 compounds (7%) when the CB6 chemical mechanism is selected. Further details on the chemical  
471 speciation profile input formats are available in the CARS user’s guide.

### 472 3.2 Spatial Allocation

473 The “**Calculate district emissions**” module calculates both total district and road link  
474 specific emissions based on road link-specific AADT data from road network GIS shapefiles. The  
475 “**Calculate district emissions**” module first gets the district total vehicle emissions (Eq. 2) based  
476 on the district-level VKTs, and then the normalized district total emissions by district weight factor,  
477  $\omega_d$  (Eq. 13). Afterwards, the normalized district total emissions are redistributed into every road  
478 link using road link-level weight factors ( $\omega_{d,t}$ ) (Eq. 15). The district total emissions from Eq. (2)  
479 and from Eq. (15) remain the same. Then the computed road link-level emissions then will be

480 converted into grid cell emissions using the modeling domain grid cell fractions computed in the  
481 “*Read\_griddesc*” function in the “**Grid4AQM**” module.

### 482 **3.3 Temporal Allocation**

483 Once chemical and spatial allocations are completed, the final step to support CTM  
484 application is a temporal allocation that converts the annual total emissions from the “**Calculate**  
485 **district emissions**” module into hourly emissions. The “*Read\_temporal*” temporal allocation  
486 function in the “**Grid4AQM**” module converts the annual emission rate ( $t\ yr^{-1}$ ) to the hourly  
487 emission rate ( $mol\ hr^{-1}$ ) using monthly, weekly, and weekday/weekend diurnal temporal profiles.  
488 This module processes these temporal profile inputs, which are the monthly (January - December),  
489 weekly (Monday - Sunday), and weekday/weekend 24-hour profile tables (0:00-23:00 LST). The  
490 users can assign these temporal profiles with a combination of vehicle, engine, fuel, and road types  
491 to enhance their temporal representations in detail.

### 492 **3.4 Chemical Transport Model Emissions**

493 The main goal of the “**Grid4AQM**” module is to generate temporally, chemically, and  
494 spatially enhanced CTM-ready gridded hourly emissions. First, it reads the CTM modeling domain  
495 configuration and then overlays it over the road network GIS shapefile and district-boundary  
496 shapefile to define the modeling domain. This overlaying process between the road network,  
497 district boundary GIS shapefiles, and modeling domain allows the “**Grid4AQM**” module to  
498 compute the fraction of road links that intersects with each grid cell. Figure 6 demonstrates how  
499 the district boundary and road network GIS shapefiles are used to perform the spatial allocation  
500 processes in CARS. Figure 6a is a native road link shapefile of Seoul with AADT, VKT, district  
501 ID, and road type. Figure 6b presents an overlay of two districts’ road links (purple and blue) over  
502 the selected region. State total emissions will be renormalized into weighed district total emission  
503 data and then redistributed into the road link. Figure 6c illustrates how the weighted road link-  
504 level emissions get allocated into modeling grid cells for CTMs. The link-level VKT ( $VKT_{d,r,l}$ )  
505 from Eq. (12) will be used to compute a total of traffic activity fractions by grid cell and then use  
506 that to assign the link-level emissions from Eq. (2) into each grid cell. When a road link intersects  
507 with multiple grid cells, the “**Grid4AQM**” module will weigh the emissions by the length of the  
508 link that intersects with each grid cell. It should be noted that current CARS model can only  
509 generate the Community Multiscale Air Quality (CAMQ)-ready gridded hourly emissions in  
510 format of IOAPI (Input/Output Applications Programming Interface) based on NetCDF format.

511 Through the overlay process, the CARS model can generate various types of output data,  
512 such as total district emissions, link-level emissions, and CTM-ready gridded emissions. For  
513 example, the CO vehicle emissions from the Seoul metropolitan in South Korea are presented in  
514 three different output formats in Fig. 7. Figure 7a shows the annual mobile  $PM_{2.5}$  emissions by

515 district. The road link level annual emissions are presented in Fig. 7b. Furthermore, the CARS  
516 applies the link-level emissions from Fig. 7b to generate the hourly grid cell emission data with a  
517 1 km × 1 km resolution for the CTM in Fig. 7c.

### 518 **3.5 National Control Strategy Application**

519 One of the unique features in the CARS compared to other mobile emissions models is that  
520 it can promptly develop a strategy to control automobile emissions in response to national  
521 emergency high PM<sub>2.5</sub> episodes. It is very common to experience high PM<sub>2.5</sub> episodes, especially  
522 during the wintertime in South Korea due to domestic and international primary and secondary air  
523 pollutants emissions. When the 72-hour forecasted PM<sub>2.5</sub> concentration exceeds the average 50  
524 μg/m<sup>3</sup> (0:00-16:00 LST), the national PM<sub>2.5</sub> emergency control strategy is activated for ten days.  
525 It applies a nationwide vehicle restriction policy within 24 hours. It enforces a limit on what kind  
526 of vehicles can be operated on a certain date. The restrictions can be closures of public parks and  
527 government facilities and of certain vehicles based on their fuel type and age, which is a major  
528 factor of engine deterioration. This policy will limit the number of vehicles on the network roads  
529 significantly, which could reduce primary PM<sub>2.5</sub> and precursor pollutant (NO<sub>x</sub>, NH<sub>3</sub>, and VOC)  
530 emissions, especially from heavily populated metropolitan regions (Choi et al., 2014; Kim et al.,  
531 2017a; Kim et al., 2017b; Kim et al., 2017c).

532 To understand the impacts of an even or odd vehicle number restriction policy in real-time,  
533 we need to quickly develop a rapid controlled response emissions for the air quality forecast  
534 modeling system based on the reduced number of vehicles on the road. The process of generating  
535 the controlled mobile emission inventory can take a long time if we start fresh. Thus, we have  
536 implemented this control strategy as an optional “**Control Factors**” function in the “**Calculate**  
537 **district emissions**” in the module for users to quickly and easily generate the controlled mobile  
538 emission inventory with consideration of the limited number of vehicles based on the vehicle,  
539 engine, fuel, and vehicle manufactured year. A one hundred percent (100%) control factor means  
540 that there are no emissions from those selected vehicles.

541 Because of the modularization system in the CARS, we can bypass some computationally  
542 expensive data processing modules (i.e., “**Process activity data**”, “**Process emission factors**”,  
543 and “**Process shape file**”) and let the “**Calculate district emissions**” module quickly apply control  
544 factors while it computes the district-level mobile emission inventory from Eq. (2). This will allow  
545 users to reduce the computational time to generate the controlled mobile emissions under a specific  
546 control scenario and develop the controlled CTM-ready gridded hourly emissions using the  
547 “**Grid4AQM**” module.



### 548 **3.6 Computational Time**

549 While the CARS can generate a high-quality spatiotemporal emission inventory, it is quite  
550 critical for the CARS to generate them effectively and accurately without being at the expense of  
551 computational time. This is especially important to meet the needs for an air quality forecast  
552 modeling system responding to a national emergency control strategy implementation.

553 In this section, we will discuss the details of the CARS computational modeling performance.  
554 While the CARS model has been highly optimized, the modularization of CARS has also improved  
555 its modeling performance with its optional module runs. The breakdown of module specific  
556 computational time estimates based on the benchmark CARS runs are listed in Table 1. The  
557 benchmark CARS case includes a total of 24,383,578 daily VKT datasets from KSTA over two  
558 different years, 84,608 emission factors for all pollutants across a combination of vehicle-age-  
559 engine-fuel types, 385,795 road links from the GIS road network shapefiles, 5,150 districts/16-  
560 states boundary GIS shapefile, and 5,494 grid cells (=82 rows and 67 columns) for CTMs. Without  
561 any computational parallelization, the total processing time of all six modules usually takes around  
562 a half hour to generate a single day CTM-ready gridded hourly emission file. However, it can be  
563 further shortened to 25-30 minutes on a higher performance computer. Because of the modular  
564 system implemented in the CARS, generating one month (31 days) long gridded hourly emissions  
565 from CTMs in 100 minutes on high-performance computers. The maximum usage of RAM can  
566 reach up to 11 GB. Table 1 shows the breakdown of computational time by each module from two  
567 different hardwares (desktop and laptop computers). The numbers in parentheses beside the  
568 “Grid4AQM” module is the computational time for a single day versus 31 days. While the  
569 “Grid4AQM” module takes an average of 4.9 minutes for a single day emissions generation,  
570 processing a consecutive 31 days saves 46% more time, decreasing it from 151.9 minutes (=4.9  
571 minutes \* 31 days) to 81.6 minutes.

## 572 **4 Results**

### 573 **CARS and CAPSS Comparison**

574 The CARS model calculates the 2015 onroad automobile emissions based on the latest  
575 2015 emission factors and the 2015-2017 vehicle activity database in South Korea. The annual  
576 total emissions from CARS are compared against the ones from NIER’s CAPSS in Table 2. The  
577 CARS model estimated the following annual total emissions in units of metric tons per year (t yr<sup>-1</sup>):  
578 NO<sub>x</sub> (301,794); VOC (61,186); CO (373,864), NH<sub>3</sub> (12,453); PM<sub>2.5</sub> (10,108), and SO<sub>x</sub> (172.0).  
579 Compared to NIER’s CAPSS, the CARS underestimated NO<sub>x</sub> (-18% decrease) and SO<sub>x</sub> (-17%  
580 decrease), and overestimated the emissions of VOC by 33%, PM<sub>2.5</sub> by 15%, CO by 52%, and NH<sub>3</sub>  
581 by 24%. Both NIER’s CAPSS and CARS shared the same emission factor tables, which hold over

582 84,608 emission factors for all pollutants across a combination of vehicle, age, engine, and fuel  
583 types.

584 The difference in results between CAPSS and CARS are caused by three following reasons.  
585 First, the number of vehicles used in CARS is slightly higher (6%) than CAPSS data (1.3 out of  
586 23 million), as well as other key traffic-related activity inputs (i.e., vehicle age distribution,  
587 averaged speed distribution, etc). Secondly, the vehicle speed information assigned by vehicle and  
588 road type play a critical role. The CAPSS calculation was based on the road-specific a single  
589 average speed value or 80% of the speed limit of the road as an input of vehicle operating speed  
590 for three road types (rural, urban, and expressway) (Lee et al., 2011b). In other words, CAPSS  
591 only assigns a “single-speed value” for each road type, and does not encounter the variation of  
592 vehicle speed during its operation on roads into the emissions calculation. Most running exhaust  
593 emissions occur during a vehicle’s low-speed operation due to its incomplete combustion of fuel,  
594 and it is critical to accurately represent the emissions across various speed bins in order to compute  
595 the accurate emissions (Fig. 4). A detailed analysis of the impact of vehicle speed will be discussed  
596 later in this chapter. Lastly, other advanced processes in the CARS, such as link-level AADT and  
597 district-level vehicle data (5,150 districts in South Korea) can reflect more spatial detail and  
598 variation than the CAPSS. The CAPSS only considers state-level data (17 states in South Korea)  
599 and five road types (interstate expressway, urban highway, rural highway, urban local, and rural  
600 local).

601 Figure 8 illustrates more details about the difference in annual emissions between CARS  
602 and CAPSS by pollutants and vehicle types. Sedan vehicles show the largest increase of VOC  
603 (33%), CO (41%), and NH<sub>3</sub> (23%) in the CARS relative to CAPSS because almost 56% of total  
604 vehicle count (13.5 million) is composed of sedan vehicles (Appendix B). In Table 3, sedan  
605 vehicles contribute 51% of total VOC and 61% of total CO annual emissions. The VOC and CO  
606 emissions from sedans are largely affected by the average speed distribution process when  
607 compared to other vehicle types. Similarly, the largest decreases of NO<sub>x</sub> (-16%) and SO<sub>x</sub> (-18%)  
608 are from trucks because they are significant NO<sub>x</sub> (~50%) and SO<sub>x</sub> contributors (~27%) and their  
609 emission factors are sensitive to vehicle speed.

## 610 **Onroad Emissions Analysis**

611 The CARS is a bottom-up emissions model, which utilizes local individual vehicle activity  
612 data, detailed local emission factors for every vehicle and fuel type, and localized inputs such as  
613 average speed distribution by road type and deterioration factor. It allows users to assess a detailed  
614 breakdown of localized emission contributions. Table 3 represents the individual air pollutants  
615 (NO<sub>x</sub>, VOC, PM<sub>2.5</sub>, CO, NH<sub>3</sub>, and SO<sub>x</sub>) emission contributions (t yr<sup>-1</sup>), fractions (%), and impact  
616 factors (IF) by the vehicle type and fuel system. The IF is defined by the normalized annual  
617 emissions with vehicle counts of each category (kg yr<sup>-1</sup> per vehicle). The CARS also can provide

618 the average daily VKT per vehicle, which is the total daily VKT divided by vehicle numbers, to  
619 explain the emission contributions in Appendix D.

620 Diesel-fueled vehicles contribute the most NO<sub>x</sub> emissions at over 85.3% (257,305 t yr<sup>-1</sup>),  
621 although the number of diesel vehicles only amounts to approximately 35% of the total vehicles  
622 (Table 3a). While diesel trucks emitted 49.1% (148,246 t yr<sup>-1</sup>) of total NO<sub>x</sub> with an IF value of  
623 47.9 (kg yr<sup>-1</sup>), the highest impact (IF = 340 kg yr<sup>-1</sup>) occurred from diesel buses with only an 8.51%  
624 contribution to the total NO<sub>x</sub> emissions. This is caused by the highest average daily VKT from  
625 diesel buses compared to other vehicles, which is expected in a highly populated metropolitan area  
626 like Seoul, South Korea. A diesel bus generally has a 3-5 times higher daily VKT (180 km d<sup>-1</sup>)  
627 than other common vehicles (gasoline sedan: 34 km d<sup>-1</sup>, diesel truck: 57 km d<sup>-1</sup>). The second-  
628 largest vehicle type is the CNG (compressed natural gas) bus (248 kg yr<sup>-1</sup>), which also has a high  
629 VKT at an average daily of 212 km d<sup>-1</sup> with only a 3.1% NO<sub>x</sub> contribution.

630 For VOC emissions, over 12 million gasoline vehicles cause 52.1% (31,885 t yr<sup>-1</sup>) of the  
631 total VOC emissions, with the gasoline sedan as the highest contributor (46.5% at 14,070 t yr<sup>-1</sup>)  
632 across all vehicle types (Table 3b). Diesel vehicles only contribute 23.0% (14,070 t yr<sup>-1</sup>) of the  
633 total VOC emissions. The IF values from VOC indicate that CNG buses have the highest, which  
634 is 247 kg yr<sup>-1</sup> (19% over total VOC) with a low number of heavy CNG vehicles. The IF of the  
635 CNG bus is the highest which is 320 kg yr<sup>-1</sup> and emits 19.5% of the total VOC. Comparing the IFs  
636 of buses across fuel types, the CNG bus emits less NO<sub>x</sub> but higher VOC than a diesel vehicle. Each  
637 CNG bus has about 33 times higher IF of VOC (320 kg yr<sup>-1</sup>) than a diesel bus (9.51 kg yr<sup>-1</sup>), and  
638 CNG buses release slightly lower NO<sub>x</sub> (248 kg yr<sup>-1</sup>) than diesel buses (340 kg yr<sup>-1</sup>) (Table 3a and  
639 3b).

640 The South Korea NIER currently does not have the PM emission factors from tire and  
641 brake wear, which are the highest contributors of PM<sub>2.5</sub> emissions from onroad vehicles (Hugo  
642 A.C. et al., 2013; Fulvio Amato et al., 2014). Once the emission factors of tire and brake wear are  
643 prepared, those emissions can be computed by CARS. For that reason, diesel vehicles become the  
644 major source of PM<sub>2.5</sub> emissions, which contributes over 98.5% (9,959 t yr<sup>-1</sup>) of the PM<sub>2.5</sub>  
645 emissions based on the CARS 2015 emissions (Table 3c). The diesel truck, SUV, and van are three  
646 major sources of total PM<sub>2.5</sub> at 53.6%, 21.4%, and 11.2%, respectively. Although over 52% of the  
647 vehicles are gasoline vehicles, their primary PM<sub>2.5</sub> contribution is limited to 1.44%. The diesel  
648 bus has the highest IF (2.83 kg yr<sup>-1</sup>), which is caused by the largest average daily VKTs.

649 Similar to VOC emissions, CO is mostly emitted through the tailpipe due to incomplete  
650 internal combustion of fuel and share similar emissions distributions across vehicle and fuel types  
651 (Table 3d). Gasoline vehicles contribute most of the CO (220,390 t yr<sup>-1</sup>, 59.0%), and sedan vehicles  
652 are the primary source (178,121 t yr<sup>-1</sup>, 47.6%) of this out of all gasoline vehicles. Across vehicle  
653 types, buses show the highest IF of CO (81.2 kg yr<sup>-1</sup>) due to its largest daily VKT. CO is the most  
654 abundant pollutant released from vehicles (373,864 t yr<sup>-1</sup>) across all pollutants from onroad

655 automobile sources. Although CO is much less reactive than other vehicle VOCs (Rinke and  
656 Zetzsch, 1984; Liu and Sander, 2015), CO emissions play a critical role in generating 30% of all  
657 hydroperoxyl radicals ( $\text{HO}_2$ ) and cause ozone formation in urban areas (Pfister et al., 2019). Thus,  
658 CO is also another crucial precursor to ozone formation in urban areas.

659  $\text{SO}_x$  emissions are related to the sulfur content within the fuel component. Diesel has the  
660 highest sulfur content than any other fuels and consequently most  $\text{SO}_x$  is contributed by diesel  
661 vehicles ( $93.8 \text{ t yr}^{-1}$ , 54.5%) (Table 3e). Within diesel vehicles, trucks provide 26.5% of  $\text{SO}_x$  ( $45.$   
662  $\text{t yr}^{-1}$ ). Although the  $\text{SO}_x$  from sedan vehicles are slightly higher ( $\sim 3.3\%$ ) than diesel trucks, the  
663 number of diesel trucks is only 29.6% of the number of gasoline sedans. Thus, diesel trucks have  
664 a higher IF than gasoline sedans. Across vehicle types, buses have the highest IF ( $0.095 \text{ kg yr}^{-1}$ )  
665 of  $\text{SO}_x$ , and diesel buses in particular have the largest IF at  $0.143 \text{ kg yr}^{-1}$ .

666 The  $\text{NH}_3$  emissions table (table 3f) indicates that 98.7% of  $\text{NH}_3$  is from gasoline vehicles  
667 while diesel trucks only contribute 1.13%. The IF result also shows that the gasoline sedan has the  
668 most significant impact per vehicle ( $1.17 \text{ kg yr}^{-1}$ ).

669 According to the vehicle activity and the CARS model results, nearly half of the total  
670 vehicles (24.3 million) are gasoline sedans (10.4 million, 42.8%), and gasoline sedan vehicles  
671 contribute the majority of VOC and CO emissions (46.5% and 47.6%), but only 7.7% of the total  
672  $\text{NO}_x$  emissions. The number of diesel vehicles is at 8.6 million (35.4%); however, they emit about  
673 85.3% of the total  $\text{NO}_x$  and 98.5% of the primary  $\text{PM}_{2.5}$ . These results indicate that the annual  
674 traffic-related automobile emissions are not only affected by the number of vehicles, but also by  
675 vehicle and fuel types and age of vehicles. Therefore, this study normalized the annual emissions  
676 by the number of vehicles to confirm the emission composition by individual vehicle types.

### 677 **Average Speed Impact Study**

678 The CARS can also optionally apply the average speed distribution (ASD) by road type to  
679 compute more realistic mobile emissions on the road network when compared to using a current  
680 single average speed value for each road type (Appendix E). Applying the ASD will generate a  
681 better representation of actual traffic patterns from each road type. To understand the impacts of  
682 ASD application, we performed sensitivity runs between using a single speed to the ASD  
683 application (Appendix F). The ASD data was described in Fig. 4, and the road-specific average  
684 single speed values were developed based on the weighted average method using the same ASD  
685 data. Appendix E and S6 describe the details of ASD as well as road-specific speed values.

686 Figure 9a shows the differences in total emissions between two scenarios and is organized  
687 by pollutant. The single-speed scenario largely underestimates the emissions across all pollutants  
688 compared to the ones from the ASD scenario.  $\text{NO}_x$  (16%), VOC (40%), and CO (30%) were  
689 especially underestimated. The difference is caused by the lack of low-speed bins ( $<16 \text{ km h}^{-1}$ )  
690 representation when a single average speed approach was used. Higher emissions are emitted while

691 vehicles are operated with low-speed bins, which decreases the combustion efficiency of ICE and  
692 releases more pollutants.

693 Figure 9b shows the road-specific emissions breakdown between the ASD and single speed  
694 approaches to understand the impacts of vehicle operating speeds on onroad automobile emissions.  
695 In this figure, each color indicates the emissions percentage differences by road types. Other than  
696  $\text{NH}_3$ , the most significant discrepancies are from urban local roads, highways, and urban highways,  
697 respectively. This pattern is caused by a better presentation of low-speed conditions ( $<16 \text{ km h}^{-1}$ )  
698 in CAR simulation (Appendix C). The lower speeds cause the incomplete combustion of ICE and  
699 increase the emission rate. Also, local urban roads, highways, and urban highways have higher  
700 road VKT contributions at 17%, 18%, and 12%, respectively (Appendix C) than rural ones. A  
701 better presentation of low-speed operating vehicles from highly travelled roads (urban local, urban  
702 highway, and highway) caused these significant differences between the ASD and single-speed  
703 approaches. Although the interstate expressway has the largest VKT contribution (41%), it also  
704 has the lowest fraction of low-speed bins (2%). That is why the difference between the ASD and  
705 single speed scenarios on interstate expressways is less than 1%. In general,  $\text{NH}_3$  emission factors  
706 do not change by vehicle operating speed, so the ASD impact is quite minimal.

## 707 **5 Conclusions**

708 The CARS is a bottom-up automobile emissions model that utilizes the localized traffic-  
709 related activity and emission factors input datasets to generate high quality localized emissions  
710 inventories for policymakers, stakeholders, and research community as well as temporally and  
711 spatially enhanced hourly gridded emissions for CTMs. First, the CARS model employs the daily  
712 VKTs for all registered vehicles and the emission factors function to compute district-level total  
713 daily emissions for each vehicle. To reflect realistic traffic patterns, the CARS model computes  
714 and utilizes link-level VKTs ( $=\text{link-length} \times \text{AADT}$ ) from the road network GIS shapefiles to  
715 redistribute the original district-level total emissions into spatially enhanced road link-level  
716 emissions. It can also optionally implement a control strategy as well as road restriction rules to  
717 improve the quality of local emission inventories and meet the needs of users.

718 The CARS model is a fully modularized and computationally optimized python-based  
719 model that can effectively process a huge dataset to calculate high quality spatiotemporal county-  
720 level, road link-level, and grid cell-level mobile emissions. We believe that the implementation of  
721 the ASD into the CARS improves the representation of onroad automobile emissions from the  
722 road network when compared to a single speed for each road type. It additionally allows the CARS  
723 to have a better representation of low speed ( $<16 \text{ km h}^{-1}$ ) vehicle emissions. We believe that CARS  
724 model's versatile spatiotemporal bottom-up automobile emissions and the in-depth analysis feature  
725 can assist government policymakers and stakeholders to quickly develop responsive emission

726 strategies to South Korea's national PM<sub>2.5</sub> emergency control strategy that enforces the nationwide  
727 vehicle restriction policy within 24 hours.

### 728 **Code Availability:**

729 The source code of the CARS model public release version 1.0 can be downloaded from the  
730 Github release website:

731 <https://doi.org/10.5281/zenodo.5033314>

732

733

### 734 **Digital Object Identifier (DOI) for the CARS version 1.0:**

735 <https://doi.org/10.5281/zenodo.5033314>

736

737

### 738 **Installation Package for CARS version 1.0:**

739 The CARS version 1.0 installation package comes with the complete inputs and outputs datasets  
740 for users to confirm their proper installation on their computers and can be downloaded from the  
741 CARS version 1 used in this paper (Baek et al., 2021):

742 <https://doi.org/10.5281/zenodo.5033314>

743

744

### 745 **User's Guide Documentation:**

746 The CARS version user's guide documentation can be accessed through the the CARS version 1  
747 used in this paper (Baek et al., 2021):

748 <https://doi.org/10.5281/zenodo.5033314>

749

### 750 **Data availability:**

751 All the datasets, excel, and python scripts used in this manuscript for the data analysis are  
752 uploaded through GMD website along with a supplemental appendix document.

753

### 754 **Author contribution**

755 Dr. B.H. Baek and Dr. Jung-Hun Woo are the lead researchers in this study. Dr. Rizzieri  
756 Pedruzzi developed the source code of CARS model, Dr. Minwoo Park tested the model and  
757 provided the model input data. Dr. Chi-Tsan Wang analyzed the model results and prepared the  
758 manuscript. Younha Kim and Chul-Han Song also analyzed the model results and provided  
759 comments.

760

761

762 **Competing interests**

763 The authors declare that they have no conflict of interest.

764 **Acknowledgments**

765 This research was funded by the National Strategic Project-Fine Particle of the National Research  
766 Foundation (NRF) of Korea funded by the Ministry of Science and ICT (MSIT), the Ministry of  
767 Environment (ME), the Ministry of Health and Welfare (MOHW) (NRF-2017M3D8A1092022),  
768 and by the Korea Environmental Industry & Technology Institute (KEITI) through the Public  
769 Technology Program based on Environmental Policy Program, funded by Korea Ministry of  
770 Environment (MOE) (2019000160007).

771

772 **References**

773 Safety flare for burning combustible gas - has tangential inlet for non-flammable gas between  
774 housing and stack, in, Shell Oil Co (Shel-C).

775 Anaconda, Anaconda python: <https://www.anaconda.com/products/individual>, last access: May,  
776 1st, 2020.

777 Appel, W., Chemel, C., Roselle, S., Francis, X., Hu, R.-M., Sokhi, R., Rao, S. T., and Galmarini,  
778 S.: Examination of the Community Multiscale Air Quality (CMAQ) model performance over the  
779 North American and European domains, *Atmospheric Environment*, 53, 142–155,  
780 10.1016/j.atmosenv.2011.11.016, 2013.

781 Baek, B. H., Pedruzzi, Rizzieri, Wang, Chi-Tsan, Woo, Jung-Hun (2021). bokhaeng/CARS:  
782 CARS (Comprehensive Automobile Emissions Research Simulator) version 1.0 Public Release  
783 (CARsv1.0). Zenodo. <https://doi.org/10.5281/zenodo.5033314>

784 Baek, B. H., and Seppanen, C., SMOKE v4.8.1 Public Release (January 29, 2021). (Version  
785 SMOKEv481\_Jan2021): <http://doi.org/10.5281/zenodo.4480334>.

786 Burnett, R., Chen, H., Szyszkowicz, M., Fann, N., Hubbell, B., Pope, C. A., Apte, J. S., Brauer,  
787 M., Cohen, A., Weichenthal, S., Coggins, J., Di, Q., Brunekreef, B., Frostad, J., Lim, S. S., Kan,  
788 H., Walker, K. D., Thurston, G. D., Hayes, R. B., Lim, C. C., Turner, M. C., Jerrett, M.,  
789 Krewski, D., Gapstur, S. M., Diver, W. R., Ostro, B., Goldberg, D., Crouse, D. L., Martin, R. V.,  
790 Peters, P., Pinault, L., Tjepkema, M., van Donkelaar, A., Villeneuve, P. J., Miller, A. B., Yin, P.,  
791 Zhou, M., Wang, L., Janssen, N. A. H., Marra, M., Atkinson, R. W., Tsang, H., Quoc Thach, T.,  
792 Cannon, J. B., Allen, R. T., Hart, J. E., Laden, F., Cesaroni, G., Forastiere, F., Weinmayr, G.,  
793 Jaensch, A., Nagel, G., Concin, H., and Spadaro, J. V.: Global estimates of mortality associated  
794 with long-term exposure to outdoor fine particulate matter, *Proceedings of the National*  
795 *Academy of Sciences*, 115, 9592, 10.1073/pnas.1803222115, 2018.  
796

797 Choi, D., Beardsley, M., Brzezinski, D., Koupal, J., and Warila, J.: MOVES Sensitivity  
798 Analysis: The Impacts of Temperature and Humidity on Emissions  
799 , available at: <https://www3.epa.gov/ttn/chief/conference/ei19/session6/choi.pdf> 2017.

800 Choi, K.-C., Lee, J.-J., Bae, C. H., Kim, C.-H., Kim, S., Chang, L.-S., Ban, S.-J., Lee, S.-J., Kim,  
801 J., and Woo, J.-H.: Assessment of transboundary ozone contribution toward South Korea using



- 802 multiple source–receptor modeling techniques, *Atmospheric Environment*, 92, 118-129,  
803 <https://doi.org/10.1016/j.atmosenv.2014.03.055>, 2014.
- 804 Cohen, A. J., Brauer, M., Burnett, R., Anderson, H. R., Frostad, J., Estep, K., Balakrishnan, K.,  
805 Brunekreef, B., Dandona, L., Dandona, R., Feigin, V., Freedman, G., Hubbell, B., Jobling, A.,  
806 Kan, H., Knibbs, L., Liu, Y., Martin, R., Morawska, L., Pope, C. A., III, Shin, H., Straif, K.,  
807 Shaddick, G., Thomas, M., van Dingenen, R., van Donkelaar, A., Vos, T., Murray, C. J. L., and  
808 Forouzanfar, M. H.: Estimates and 25-year trends of the global burden of disease attributable to  
809 ambient air pollution: an analysis of data from the Global Burden of Diseases Study 2015, *The*  
810 *Lancet*, 389, 1907-1918, 10.1016/S0140-6736(17)30505-6, 2017.  
811
- 812 Dennis, R., Fox, T., Fuentes, M., Gilliland, A., Hanna, S., Hogrefe, C., Irwin, J., Rao, S. T.,  
813 Scheffe, R., Schere, K., Steyn, D., and Venkatram, A.: A FRAMEWORK FOR EVALUATING  
814 REGIONAL-SCALE NUMERICAL PHOTOCHEMICAL MODELING SYSTEMS, *Environ*  
815 *Fluid Mech (Dordr)*, 10, 471-489, 10.1007/s10652-009-9163-2, 2010.
- 816 EEA: EMEP/EEO air pollutant emission inventory guidebook 2016, 2019.
- 817 Enthought, Enthought Canapy Python: <https://assets.enthought.com/downloads/edm/>, last  
818 access: May, 1st, 2020.
- 819 Fallahshorshani, M., André, M., Bonhomme, C., and Seigneur, C.: Coupling Traffic, Pollutant  
820 Emission, Air and Water Quality Models: Technical Review and Perspectives, *Procedia - Social*  
821 *and Behavioral Sciences*, 48, 1794-1804, <https://doi.org/10.1016/j.sbspro.2012.06.1154>, 2012.
- 822 Fulvio Amato, Flemming R. Cassee, Hugo A.C. Denier van der Gon, Robert Gehrig, Mats  
823 Gustafsson, Wolfgang Hafner, Roy M. Harrison, Magdalena Jozwicka, Frank J. Kelly,  
824 TeresaMoreno, Andre S.H. Prevot, Martijn Schaap, Jordi Sunyer, Xavier Querol, Urban air  
825 quality:The challenge of traffic non-exhaust emissions, *Journal of Hazardous Materials*, 275, 31-  
826 36, <https://doi.org/10.1016/j.jhazmat.2014.04.053>, 2014.  
827
- 828 Guevara, M., Tena, C., Porquet, M., Jorba, O., and Pérez García-Pando, C.: HERMESv3, a  
829 stand-alone multi-scale atmospheric emission modelling framework – Part 1: global and regional  
830 module, *Geosci. Model Dev.*, 12, 1885-1907, 10.5194/gmd-12-1885-2019, 2019.
- 831 Hogrefe, C., Rao, S. T., Kasibhatla, P., Hao, W., Sistla, G., Mathur, R., and McHenry, J.:  
832 Evaluating the performance of regional-scale photochemical modeling systems: Part II—ozone

- 833 predictions, *Atmospheric Environment*, 35, 4175-4188, [https://doi.org/10.1016/S1352-](https://doi.org/10.1016/S1352-2310(01)00183-2)  
834 [2310\(01\)00183-2](https://doi.org/10.1016/S1352-2310(01)00183-2), 2001a.
- 835 Hogrefe, C., Rao, S. T., Kasibhatla, P., Kallos, G., Tremback, C. J., Hao, W., Olerud, D., Xiu,  
836 A., McHenry, J., and Alapaty, K.: Evaluating the performance of regional-scale photochemical  
837 modeling systems: Part I—meteorological predictions, *Atmospheric Environment*, 35, 4159-  
838 4174, [https://doi.org/10.1016/S1352-2310\(01\)00182-0](https://doi.org/10.1016/S1352-2310(01)00182-0), 2001b.
- 839 Hugo A.C. Denier van der Gon, Miriam E. Gerlofs-Nijland, Robert Gehrig, Mats Gustafsson,  
840 Nicole Janssen, Roy M. Harrison, Jan Hulskotte, Christer Johansson, Magdalena Jozwicka,  
841 Menno Keuken, Klaas Krijgsheld, Leonidas Ntziachristos, Michael Riediker & Flemming R.  
842 Cassee: The Policy Relevance of Wear Emissions from Road Transport, Now and in the  
843 Future—An International Workshop Report and Consensus Statement, *Journal of the Air &*  
844 *Waste Management Association*, 63:2, 136-149, DOI: 10.1080/10962247.2012.741055, 2013  
845
- 846 Ibarra-Espinosa, S., Ynoue, R., amp, apos, Sullivan, S., Pebesma, E., Andrade, M. d. F., and  
847 Osses, M.: VEIN v0.2.2: an R package for bottom-up vehicular emissions inventories, *Geosci.*  
848 *Model Dev.*, 11, 2209-2229, 10.5194/gmd-11-2209-2018, 2018a.
- 849 Ibarra-Espinosa, S., Ynoue, R., O'Sullivan, S., Pebesma, E., Andrade, M. D. F., and Osses, M.:  
850 VEIN v0.2.2: an R package for bottom-up vehicular emissions inventories, *Geosci. Model Dev.*,  
851 11, 2209-2229, 10.5194/gmd-11-2209-2018, 2018b.
- 852 IEMA, Inventário de Emissões Atmosféricas do Transporte Rodoviário de Passageiros no  
853 Município de São Paulo.: <http://emissoes.energiaambiente.org.br>, last access: May, 1st, 2017.
- 854 Jang, Y. K., Cho, K. L., Kim, K., Kim, H. J., and Kim, J.: Development of methodology for  
855 estimation of air pollutants emissions and future emissions from on-road mobile sources.,  
856 National Institute of Environmental Research, Incheon, Korea., available at: 2007.
- 857 Kaewunruen, S., Sussman, J. M., and Matsumoto, A.: Grand Challenges in Transportation and  
858 Transit Systems, *Frontiers in Built Environment*, 2, 10.3389/fbuil.2016.00004, 2016.
- 859 Kim, B.-U., Bae, C., Kim, H. C., Kim, E., and Kim, S.: Spatially and chemically resolved source  
860 apportionment analysis: Case study of high particulate matter event, *Atmospheric Environment*,  
861 162, 55-70, <https://doi.org/10.1016/j.atmosenv.2017.05.006>, 2017a.

- 862 Kim, H. C., Kim, E., Bae, C., Cho, J. H., Kim, B. U., and Kim, S.: Regional contributions to  
863 particulate matter concentration in the Seoul metropolitan area, South Korea: seasonal variation  
864 and sensitivity to meteorology and emissions inventory, *Atmos. Chem. Phys.*, 17, 10315-10332,  
865 10.5194/acp-17-10315-2017, 2017b.
- 866 Kim, H. C., Kim, S., Kim, B.-U., Jin, C.-S., Hong, S., Park, R., Son, S.-W., Bae, C., Bae, M.,  
867 Song, C.-K., and Stein, A.: Recent increase of surface particulate matter concentrations in the  
868 Seoul Metropolitan Area, Korea, *Scientific Reports*, 7, 4710, 10.1038/s41598-017-05092-8,  
869 2017c.
- 870 L., W. P., and Heo, G.: Development of revised SAPRC aromatics mechanism, available at:  
871 <https://www.engr.ucr.edu/~carter/SAPRC/saprc11.pdf> 2012.
- 872 Lee, D., Lee, Y.-M., Jang, K.-W., Yoo, C., Kang, K.-H., Lee, J.-H., Jung, S.-W., Park, J.-M.,  
873 Lee, S.-B., Han, J.-S., Hong, J.-H., and Lee, S.-J.: Korean National Emissions Inventory System  
874 and 2007 Air Pollutant Emissions, *Asian Journal of Atmospheric Environment*, 5-4, 278-291,  
875 2011a.
- 876 Lee, D.-G., Lee, Y.-M., Jang, K.-W., Yoo, C., Kang, K.-H., Lee, J.-H., Jung, S.-W., Park, J.-M.,  
877 Lee, S.-B., Han, J.-S., Hong, J.-H., and Lee, S.-J.: Korean National Emissions Inventory System  
878 and 2007 Air Pollutant Emissions, *Asian Journal of Atmospheric Environment*, 5,  
879 10.5572/ajae.2011.5.4.278, 2011b.
- 880 Lejri, D., Can, A., Schiper, N., and Leclercq, L.: Accounting for traffic speed dynamics when  
881 calculating COPERT and PHEM pollutant emissions at the urban scale, *Transportation Research*  
882 *Part D: Transport and Environment*, 63, 588-603, <https://doi.org/10.1016/j.trd.2018.06.023>,  
883 2018.
- 884 Li, F., Zhuang, J., Cheng, X., Li, M., Wang, J., and Yan, Z.: Investigation and Prediction of  
885 Heavy-Duty Diesel Passenger Bus Emissions in Hainan Using a COPERT Model, *Atmosphere*,  
886 10, 106, 10.3390/atmos10030106, 2019.
- 887 Li, Q., Qiao, F., and Yu, L.: Vehicle Emission Implications of Drivers Smart Advisory System  
888 for Traffic Operations in Work Zones, *Journal of the Air & Waste Management Association*, 11,  
889 10.1080/10962247.2016.1140095, 2016.
- 890 Liu, H., Guensler, R., Lu, H., Xu, Y., Xu, X., and Rodgers, M.: MOVES-Matrix for High-  
891 Performance On-Road Energy and Running Emission Rate Modeling Applications, *Journal of*  
892 *the Air & Waste Management Association*, 69, 10.1080/10962247.2019.1640806, 2019.

- 893 Liu, Y., and Sander, S. P.: Rate Constant for the OH + CO Reaction at Low Temperatures, The  
894 Journal of Physical Chemistry A, 119, 10060-10066, 10.1021/acs.jpca.5b07220, 2015.
- 895 Luo, H., Astitha, M., Hogrefe, C., Mathur, R., and Rao, S. T.: A new method for assessing the  
896 efficacy of emission control strategies, Atmospheric Environment, 199, 233-243,  
897 <https://doi.org/10.1016/j.atmosenv.2018.11.010>, 2019.
- 898 Lv, W., Hu, Y., Li, E., Liu, H., Pan, H., Ji, S., Hayat, T., Alsaedi, A., and Ahmad, B.: Evaluation  
899 of vehicle emission in Yunnan province from 2003 to 2015, J. Clean Prod., 207, 814-825,  
900 <https://doi.org/10.1016/j.jclepro.2018.09.227>, 2019.
- 901 Moussiopoulos, N., Vlachokostas, C., Tsilingiridis, G., Douros, I., Hourdakakis, E., Naneris, C.,  
902 and Sidiropoulos, C.: Air quality status in Greater Thessaloniki Area and the emission reductions  
903 needed for attaining the EU air quality legislation, Sci. Total Environ., 407, 1268-1285,  
904 <https://doi.org/10.1016/j.scitotenv.2008.10.034>, 2009.
- 905 Nagpure, A. S., Gurjar, B. R., Kumar, V., and Kumar, P.: Estimation of exhaust and non-exhaust  
906 gaseous, particulate matter and air toxics emissions from on-road vehicles in Delhi, Atmospheric  
907 Environment, 127, 118-124, 10.1016/j.atmosenv.2015.12.026, 2016.
- 908 NIER: Study on Air Pollutant Emission Estimation Method in Transportation section(II) 11-  
909 1480523-003573-01, National Archives of Korea, available at:  
910 [https://www.archives.go.kr/next/manager/publishmentSubscriptionDetail.do?prt\\_seq=114054&p](https://www.archives.go.kr/next/manager/publishmentSubscriptionDetail.do?prt_seq=114054&p)  
911 [age=1554&prt\\_arc\\_title=&prt\\_pub\\_kikwan=&prt\\_no](https://www.archives.go.kr/next/manager/publishmentSubscriptionDetail.do?prt_seq=114054&p_age=1554&prt_arc_title=&prt_pub_kikwan=&prt_no) 2018.
- 912 Ntziachristos, L., and Samaras, Z.: Speed-dependent representative emission factors for catalyst  
913 passenger cars and influencing parameters, Atmospheric Environment, 34, 4611-4619,  
914 [https://doi.org/10.1016/S1352-2310\(00\)00180-1](https://doi.org/10.1016/S1352-2310(00)00180-1), 2000.
- 915 Ntziachristos, L., Gkatzoflias, D., Kouridis, C., and Samaras, Z.: COPERT: A European road  
916 transport emission inventory model, 491-504 pp., 2009.
- 917 Pedruzzi, R., Baek, B. H., and Wang, C.-T., CARS: <https://github.com/CMASCenter/CARS>,  
918 last access: MAY, 1st, 2020.
- 919 Perugu, H., Ramirez, L., and DaMassa, J.: Incorporating temperature effects in California's on-  
920 road emission gridding process for air quality model inputs, Environ Pollut, 239, 1-12,  
921 10.1016/j.envpol.2018.03.094, 2018.

- 922 Perugu, H.: Emission modelling of light-duty vehicles in India using the revamped VSP-based  
923 MOVES model: The case study of Hyderabad, *Transportation Research Part D: Transport and*  
924 *Environment*, 68, 150-163, <https://doi.org/10.1016/j.trd.2018.01.031>, 2019.
- 925 Pfister, G., Wang, C.-t., Barth, M., Flocke, F., Vizuete, W., and Walters, S.: Chemical  
926 Characteristics and Ozone Production in the Northern Colorado Front Range, *JGR*, 2019.
- 927 Pinto, J. A., Kumar, P., Alonso, M. F., Andreão, W. L., Pedruzzi, R., dos Santos, F. S., Moreira,  
928 D. M., and Albuquerque, T. T. d. A.: Traffic data in air quality modeling: A review of key  
929 variables, improvements in results, open problems and challenges in current research,  
930 *Atmospheric Pollution Research*, 11, 454-468, <https://doi.org/10.1016/j.apr.2019.11.018>, 2020.
- 931 Rao, S. T., Galmarini, S., and Puckett, K.: Air Quality Model Evaluation International Initiative  
932 (AQMEII): Advancing the State of the Science in Regional Photochemical Modeling and Its  
933 Applications, *Bulletin of the American Meteorological Society*, 92, 23-30,  
934 10.1175/2010BAMS3069.1, 2011.
- 935 Rodriguez-Rey et al. (2021): Rodriguez-Rey, D., Guevara, M., Linares, MP., Casanovas, J.,  
936 Salmerón, J., Soret, A., Jorba, O., Tena, C., Pérez García-Pando, C.: A coupled macroscopic  
937 traffic and pollutant emission modelling system for Barcelona, *Transportation Research Part D*,  
938 92, <https://doi.org/10.1016/j.trd.2021.102725>, 2021.
- 939 Rinke, M., and Zetzsch, C.: Rate Constants for the Reactions of OH Radicals with Aromatics:  
940 Benzene, Phenol, Aniline, and 1,2,4-Trichlorobenzene, *Berichte der Bunsengesellschaft für*  
941 *physikalische Chemie*, 88, 55-62, 10.1002/bbpc.19840880114, 1984.
- 942 Russell, A., and Dennis, R.: NARSTO critical review of photochemical models and modeling,  
943 *Atmospheric Environment*, 34, 2283-2324, [https://doi.org/10.1016/S1352-2310\(99\)00468-9](https://doi.org/10.1016/S1352-2310(99)00468-9),  
944 2000.
- 945 Ryu, J. H., Han, J. S., Lim, C. S., Eom, M. D., Hwang, J. W., Yu, S. H., Lee, T. W., Yu, Y. S.,  
946 and Kim, G. H.: The Study on the Estimation of Air Pollutants from Auto- mobiles (I) -  
947 Emission Factor of Air Pollutants from Middle and Full sized Buses., in, *Transportation*  
948 *Pollution Research Center, National Institute of Environmental Research, Incheon, Korea.*, 2003.
- 949 Ryu, J. H., Lim, C. S., Yu, Y. S., Han, J. S., Kim, S. M., Hwang, J. W., Eom, M. D., Kim, G. Y.,  
950 Jeon, M. S., Kim, Y. H., Lee, J. T., and Lim, Y. S.: The Study on the Esti- mation of Air  
951 Pollutants from Automobiles (II) - Emis- sion Factor of Air Pollutants from Diesel Truck., in,

952 Trans- portation Pollution Research Center, National Institute of Environmental Research,  
953 Incheon, Korea., 2004.

954 Ryu, J. H., Yu, Y. S., Lim, C. S., Kim, S. M., Kim, J. C., Gwon, S. I., Jeong, S. W., and Kim, D.  
955 W.: The Study on the Estimation of Air Pollutants from Automobiles (III) - Emission Factor of  
956 Air Pollutants from Small sized Light-duty Vehicles., in, Transportation Pollution Research  
957 Center, National Institute of Environmental Research, Korea., 2005.

958 Sallis, P., Bull, F., Burdett, P., Frank, P., Griffiths, P., Giles-Corti, P., and Stevenson, M.: Use of  
959 science to guide city planning policy and practice: How to achieve healthy and sustainable future  
960 cities, *The Lancet*, 388, 10.1016/S0140-6736(16)30068-X, 2016.

961 Smit, R., Kingston, P., Neale, D. W., Brown, M. K., Verran, B., and Nolan, T.: Monitoring on-  
962 road air quality and measuring vehicle emissions with remote sensing in an urban area,  
963 *Atmospheric Environment*, 218, 116978, <https://doi.org/10.1016/j.atmosenv.2019.116978>, 2019.

964 Sun, W., Duan, N., Yao, R., Huang, J., and Hu, F.: Intelligent in-vehicle air quality  
965 management : a smart mobility application dealing with air pollution in the traffic, 2016.

966 Tominaga, Y., and Stathopoulos, T.: Ten questions concerning modeling of near-field pollutant  
967 dispersion in the built environment, *Build. Environ.*, 105, 390-402,  
968 <https://doi.org/10.1016/j.buildenv.2016.06.027>, 2016.

969 USEPA: Population and Activity of Onroad Vehicles in MOVES3, in, edited by: USEPA, 2020.

970 WHO, Ambient air pollution- a major threat to health and climate:  
971 <https://www.who.int/airpollution/ambient/en/>, last 2019.

972 Xu, X., Liu, H., Anderson, J. M., Xu, Y., Hunter, M. P., Rodgers, M. O., and Guensler, R. L.:  
973 Estimating Project-Level Vehicle Emissions with Vissim and MOVES-Matrix, *Transportation*  
974 *Research Record*, 2570, 107-117, 10.3141/2570-12, 2016.

975 Yarwood, G., and Jung, J.: UPDATES TO THE CARBON BOND MECHANISM FOR  
976 VERSION 6 (CB6), 2010.  
977

978 **Tables**

979 **Table 1.** Computational processing time by CARS module based on the modeling setup: Total  
 980 number of activity data = 24,383,578; Emission Factors = 84,608; GIS road links=385,795;  
 981 districts/states=5,150/16; 9km×9km grid cells=5,494 (82 columns× 67 columns).

No	Module	Desktop i7 (minutes)	Laptop i9 (minutes)	Averaged Time (minutes)
1	<b>Process activity data</b>	1.8	1.5	1.7
2	<b>process emission factors</b>	1.1	0.8	1.0
3	<b>Process shape file</b>	9.9	7.3	8.6
4	<b>Calculate district emissions</b>	6.4	5.7	6.1
5	<b>Grid4AQM [31days]</b>	4.8 [75.9]	5.0 [87.2]	4.9 [81.6]
6	<b>Plot figures</b>	6.2	5.4	5.8
<b>Total [31days]</b>		<b>30.2 [101.3]</b>	<b>25.7 [107.9]</b>	<b>28.1[104.8]</b>

982

983

984

985 **Table 2.** The total emissions comparison between CARS and CAPSS for the 2015 emission.

Emission Inventory	Pollutants (t yr <sup>-1</sup> )					
	NO <sub>x</sub>	VOC	PM2.5	CO	SO <sub>x</sub>	NH <sub>3</sub>
CARS 2015	<b>301,794</b>	<b>61,186</b>	<b>10,108</b>	<b>373,864</b>	<b>172</b>	<b>12,453</b>
CAPSS 2015	369,585	46,145	8,817	245,516	209	10,079

986

987



988 **Table 3.** The summary tables of emissions (t yr<sup>-1</sup>), contributions (%), and impact factor (IF, kg yr<sup>-1</sup>) per vehicle for criteria air pollutants (CAPs) by vehicle and fuel types: (a) for NO<sub>x</sub>; (b) VOC;  
 989  
 990 (c) for PM<sub>2.5</sub>; (d) for CO; (e) for SO<sub>x</sub>; and (f) for NH<sub>3</sub>.

991  
 992 (a) NO<sub>x</sub>

Vehicle	Gasoline		Diesel		LPG		CNG		Hybrid		Total	
	Emission	IF	Emission	IF	Emission	IF	Emission	IF	Emission	IF	Emission	IF
Sedan	20,219 (6.70%)	1.94	14,783 (4.90%)	12.8	8,159 (2.77%)	4.49	12 (0.00%)	1.26	65 (0.02%)	0.39	43,239 (14.3%)	3.19
Truck	23 (0.01%)	5.54	<b>148,246 (49.1%)</b>	47.9	920 (0.31%)	4.55	88 (0.03%)	66.4	-	-	<b>149,277 (49.5%)</b>	45.2
Bus	0 (0.00%)	0.97	25,677 (8.51%)	<b>340</b>	-	-	9,260 (3.07%)	248	0 (0.00%)	1.77	34,938 (11.6%)	<b>333</b>
SUV	159 (0.05%)	1.19	39,565 (13.1%)	11.4	175 (0.06%)	8.54	0 (0.00%)	1.60	1 (0.00%)	0.42	39,900 (13.2%)	11.0
Van	14 (0.00%)	4.78	16,659 (5.52%)	22.6	1,337 (0.44%)	6.80	0 (0.00%)	1.25	0 (0.00)	0.37	18,012 (6.00%)	19.2
Taxi	-	-	-	-	1,217 (0.40%)	2.11	-	-	-	-	1,217 (0.40%)	2.11
Special	1 (0.00%)	20.1	12,347 (4.10%)	152	0 (0.00%)	0.52	-	-	-	-	12,375 (4.10%)	151
Motorcycle	2,836 (0.94%)	1.31	-	-	-	-	-	-	-	-	2,836 (0.94%)	1.32
Total	23,253 (7.70%)	1.83	<b>257,305 (85.3%)</b>	29.9	11,809 (3.91%)	4.20	9,361 (3.10%)	<b>36.7</b>	66 (0.02%)	0.39	301,794 (100%)	13.3

993  
 994 (b) VOC

Vehicle	Gasoline		Diesel		LPG		CNG		Hybrid		Total	
	Emission	IF	Emission	IF	Emission	IF	Emission	IF	Emission	IF	Emission	IF
Sedan	28,434 (46.5%)	2.73	629 (1.03%)	0.55	2,107 (3.44%)	1.16	3 (0.01%)	0.33	77 (0.13%)	0.47	<b>31,250 (51.1%)</b>	2.30
Truck	23 (0.04%)	5.44	8,194 (13.4%)	2.65	286 (0.47%)	1.41	102 (0.17%)	77.2	-	-	8,605 (14.1%)	2.61
Bus	0 (0.00%)	1.65	717 (1.17%)	9.51	-	-	11,942 (19.5%)	320	0 (0.00%)	0	12,659 (20.7%)	<b>112</b>
SUV	246 (0.40%)	1.84	2,441 (3.99%)	0.71	46 (0.08%)	2.25	0 (0.00%)	0.75	1 (0.00%)	0.55	2,733 (4.47%)	0.76
Van	21 (0.03%)	7.04	1,185 (1.94%)	1.61	393 (0.64%)	2.00	0 (0.00%)	0.45	0 (0.00%)	0	1,599 (2.61%)	1.71
Taxi	-	-	-	-	273 (0.45%)	0.47	-	-	-	-	273 (0.45%)	0.47
Special	1 (0.00%)	25.8	904 (1.48%)	11.1	0 (0.00%)	0.23	-	-	-	-	905 (1.48%)	11.0
Motorcycle	3,160 (5.16%)	1.46	-	-	-	-	-	-	-	-	3,160 (5.16%)	1.46
Total	<b>31,885 (52.1%)</b>	2.50	14,070 (23.0%)	1.64	3,106 (5.08%)	1.10	12,047 (19.7%)	<b>247</b>	78 (0.13%)	0.47	61,186 (100%)	2.51

995  
 996 (c) PM<sub>2.5</sub>

Vehicle	Gasoline		Diesel		LPG		CNG		Hybrid		Total	
	Emission	IF	Emission	IF	Emission	IF	Emission	IF	Emission	IF	Emission	IF
Sedan	144 (1.42%)	0.01	809 (8.00%)	0.70	0	0	0	0	3 (0.03%)	0.02	956 (9.46%)	0.07
Truck	0 (0.01%)	0	<b>5,415 (53.6%)</b>	1.75	0	0	0	0	-	-	<b>5,415 (53.6%)</b>	1.64
Bus	0	0	214 (2.11%)	<b>2.83</b>	-	-	0	0	0 (0.01%)	0.09	214 (2.11%)	1.89
SUV	2 (0.02%)	0.02	2,165 (21.4%)	0.63	0	0	0	0	0	0.02	2,167 (21.4%)	0.60
Van	0	0	1,127 (11.2%)	1.53	0	0	0	0	0	0.02	1,127 (11.2%)	1.20
Taxi	-	-	-	-	0	0	-	-	-	-	0	0
Special	0	0	230 (2.28%)	2.82	0	0	-	-	-	-	230 (2.28%)	<b>2.81</b>
Motorcycle	0	0	-	-	-	-	-	-	-	-	0	0
Total	146 (1.44%)	0.01	<b>9,959 (98.5%)</b>	<b>1.16</b>	0	0	0	0	3 (0.03%)	0.02	10,108 (100%)	0.41

997  
 998

999

1000 (d) CO

Vehicle	Gasoline		Diesel		LPG		CNG		Hybrid		Total	
	Emission	IF	Emission	IF	Emission	IF	Emission	IF	Emission	IF	Emission	IF
Sedan	178,121 (47.6%)	17.1	3,436 (0.92%)	2.98	42,886 (11.5%)	23.6	29 (0.01%)	2.91	177 (0.05%)	1.07	<b>224,649 (60.1%)</b>	16.6
Truck	254 (0.07%)	61.1	47,065 (12.6%)	15.2	9,088 (2.43%)	44.9	68 (0.02%)	51.4	-	-	56,475 (15.1%)	17.1
Bus	0 (0.00%)	19.3	7,633 (2.05%)	<b>101</b>	-	-	1542 (0.41%)	41.3	1 (0.00%)	4.64	9,176 (2.45%)	<b>81.2</b>
SUV	2,616 (0.70%)	19.6	13,401 (3.58%)	3.87	791 (0.21%)	38.6	0 (0.00%)	4.09	2 (0.00%)	1.15	16,808 (4.50%)	4.65
Van	131 (0.04%)	43.4	6,611 (1.77%)	8.97	8,032 (2.15%)	40.9	2 (0.00%)	6.53	0 (0.00%)	1.00	14,777 (3.95%)	15.8
Taxi	-	-	-	-	8,481 (2.27%)	14.7	-	-	-	-	8,481 (2.27%)	14.7
Special	13 (0.00%)	269	4,224 (1.13%)	51.7	1 (0.00%)	3.69	-	-	-	-	4,239 (1.13%)	51.7
Motorcycle	39,256 (10.5%)	18.2	-	-	-	-	-	-	-	-	39,256 (10.5%)	18.2
<b>Total</b>	<b>220,390 (59.0%)</b>	<b>17.3</b>	<b>82,372 (22.0%)</b>	<b>9.57</b>	<b>69,281 (18.5%)</b>	<b>24.6</b>	<b>1641 (0.44%)</b>	<b>33.6</b>	<b>180 (0.05%)</b>	<b>1.07</b>	<b>373,864 (100%)</b>	<b>15.4</b>

1001

1002 (e) SO<sub>x</sub>

Vehicle	Gasoline		Diesel		LPG		CNG		Hybrid		Total	
	Emission	IF	Emission	IF	Emission	IF	Emission	IF	Emission	IF	Emission	IF
Sedan	51.3 (29.8%)	0.005	6.5 (3.79%)	0.006	8.28 (4.81%)	0.005	0	0	1.14 (0.67%)	0.007	<b>67.2 (39.1%)</b>	0.005
Truck	0.03 (0.02%)	0.008	45.5 (26.5%)	0.015	0.97 (0.57%)	0.005	0	0	-	-	46.5 (27.1%)	0.014
Bus	0 (0.00%)	0.003	10.8 (6.26%)	<b>0.143</b>	-	-	0	0	0.01 (0.01%)	0.047	10.8 (6.26%)	<b>0.095</b>
SUV	0 (0.00%)	0.000	18.2 (10.6%)	0.005	0.00 (0.00%)	0.000	0	0	0.01 (0.01%)	0.007	18.2 (10.6%)	0.005
Van	0.02 (0.01%)	0.006	5.5 (3.20%)	0.007	0.77 (0.45%)	0.004	0	0	0 (0.00%)	0.010	6.30 (3.66%)	0.007
Taxi	-	-	-	-	7.71 (4.49%)	0.013	-	-	-	-	7.71 (4.48%)	0.013
Special	0 (0.00%)	0.003	7.3 (4.27%)	0.090	0.00 (0.00%)	0.005	-	-	-	-	7.34 (4.27%)	0.090
Motorcycle	7.94 (4.62%)	0.004	-	-	-	-	-	-	-	-	7.94 (4.62%)	0.004
<b>Total</b>	<b>59.3 (34.5%)</b>	<b>0.006</b>	<b>93.8 (54.5%)</b>	<b>0.011</b>	<b>17.7 (10.3%)</b>	<b>0.006</b>	<b>0</b>	<b>0</b>	<b>1.17 (0.68%)</b>	<b>0.007</b>	<b>172 (100%)</b>	<b>0.007</b>

1003

1004

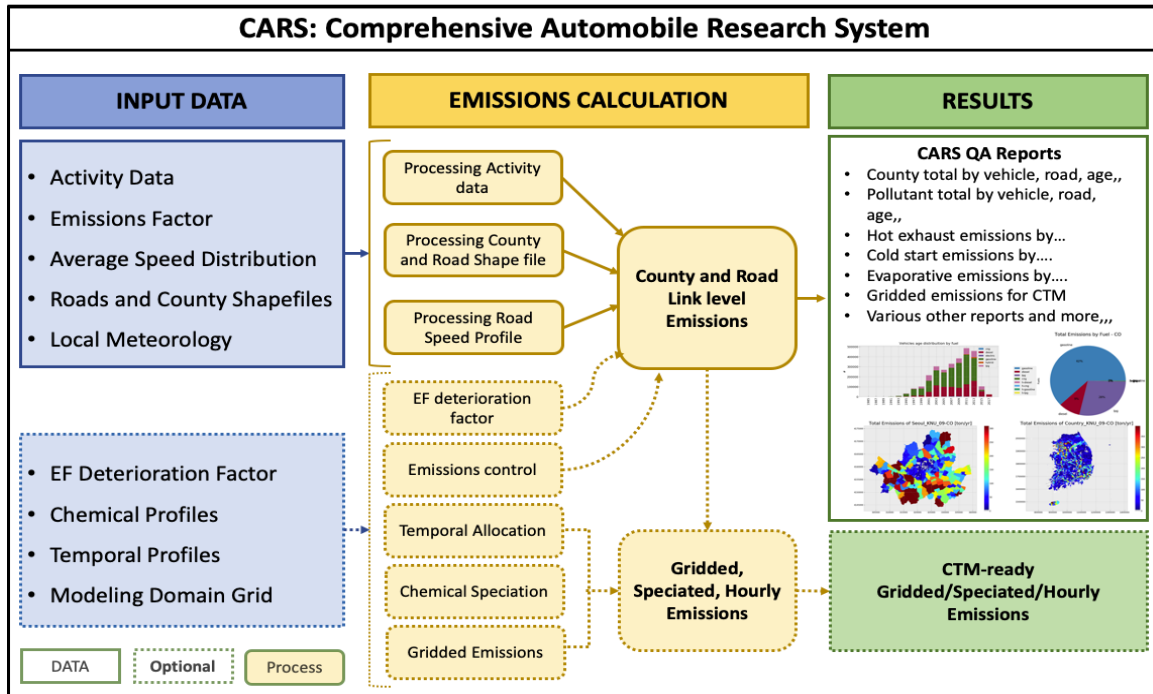
1005 (e) NH<sub>3</sub>

Vehicle	Gasoline		Diesel		LPG		CNG		Hybrid		Total	
	Emission	IF	Emission	IF	Emission	IF	Emission	IF	Emission	IF	Emission	IF
Sedan	12,225 (98.3%)	<b>1.17</b>	20 (0.16%)	0.02	0	0.00	0	0	19 (0.15%)	0.11	<b>12,284 (98.6%)</b>	<b>0.91</b>
Truck	0 (0.00%)	0.03	82 (0.66%)	0.03	0	0.00	0	0	-	-	82 (0.66%)	0.02
Bus	0 (0.00%)	0.09	15 (0.12%)	0.19	-	-	0	0	0 (0.00%)	0.51	15 (0.12%)	0.13
SUV	0 (0.00%)	0.00	0 (0.00%)	0.00	0	0.00	0	0	0 (0.00%)	0.16	0 (0.00%)	0.00
Van	0 (0.00%)	0.02	14 (0.11%)	0.02	0	0.00	0	0	0 (0.00%)	0.09	14 (0.11%)	0.01
Taxi	-	-	-	-	0	0.00	-	-	-	-	0 (0.00%)	0.00
Special	0 (0.00%)	0.01	10 (0.08%)	0.12	0	0.00	-	-	-	-	10 (0.08%)	0.12
Motorcycle	49 (0.39%)	0.02	-	-	-	-	-	-	-	-	49 (0.39%)	0.02
<b>Total</b>	<b>12,293 (98.7%)</b>	<b>0.97</b>	<b>141 (1.13%)</b>	<b>0.02</b>	<b>0</b>	<b>0.00</b>	<b>0</b>	<b>0</b>	<b>19 (0.16%)</b>	<b>0.12</b>	<b>12,453 (100%)</b>	<b>0.51</b>

1006

1007

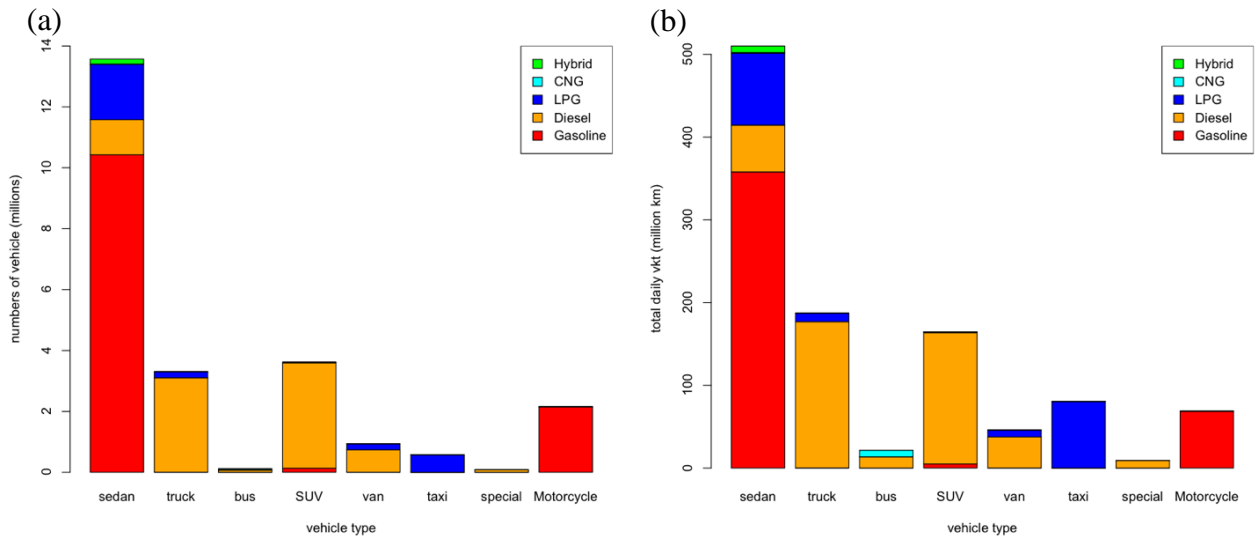
1008 **Figures**



1009

1010 **Figure 1.** CARS schematic methodology to estimate mobile emissions.

1011



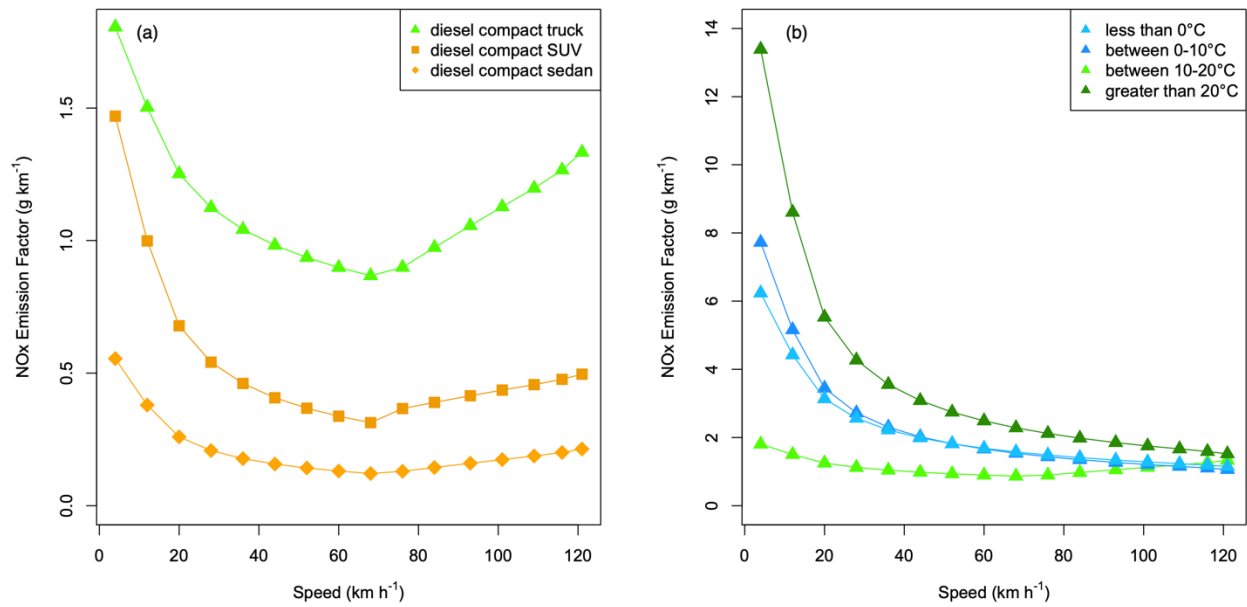
1012

1013 **Figure 2.** (a) The number of vehicles by vehicle and fuel types and (b) the total daily VKT by

1014 vehicle and fuel types in South Korea.

1015

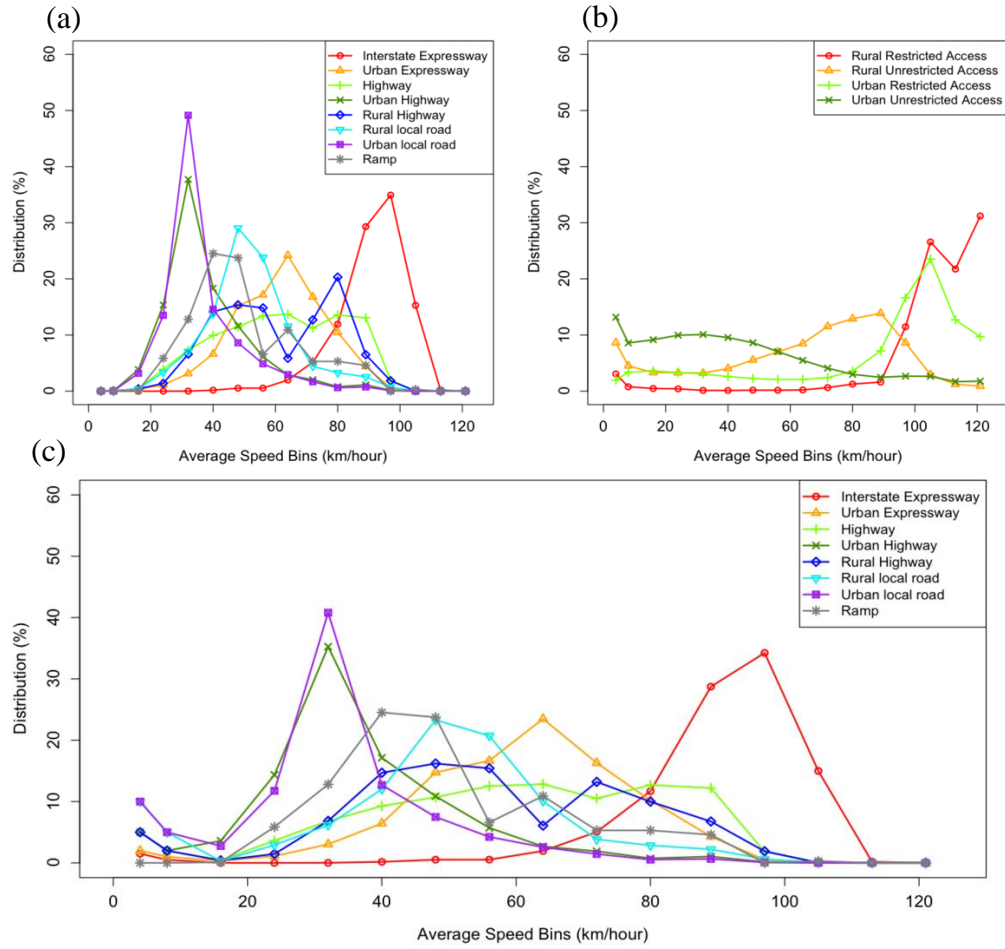
1016



1017

1018 **Figure 3.** Variation of NO<sub>x</sub> emission factors from diesel compact engines by vehicle speed and  
 1019 ambient temperatures: **(a)** NO<sub>x</sub> emission factors function to vehicle speed; **(b)** NO<sub>x</sub> emission  
 1020 factors of diesel compact truck function to vehicle speed and ambient temperature.

1021



1022

1023

1024

1025

1026

1027

1028

**Figure 4.** (a) The South Korea speed distribution by road types. (b) The Georgia state speed distribution by road types. (c) The average speed distribution (ASD) by road types used in this study for South Korea.

1029  
1030  
1031

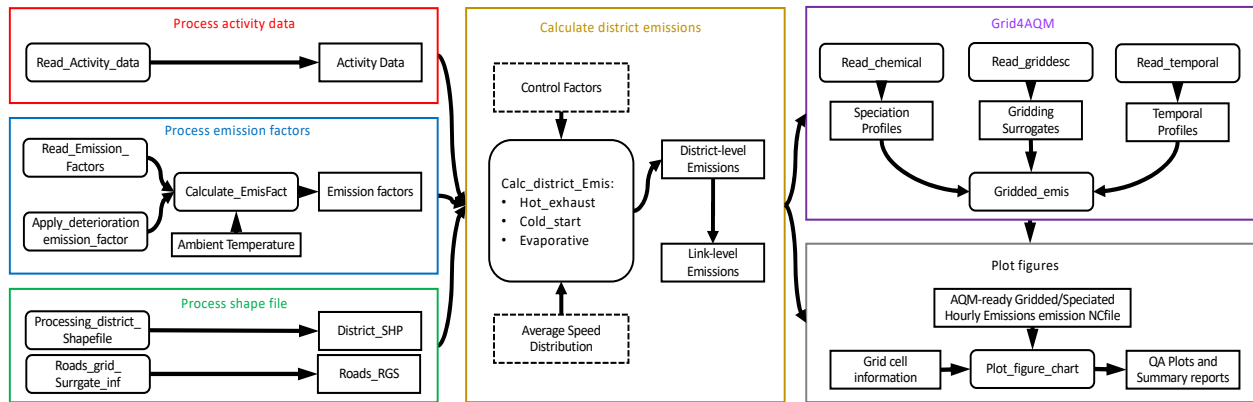
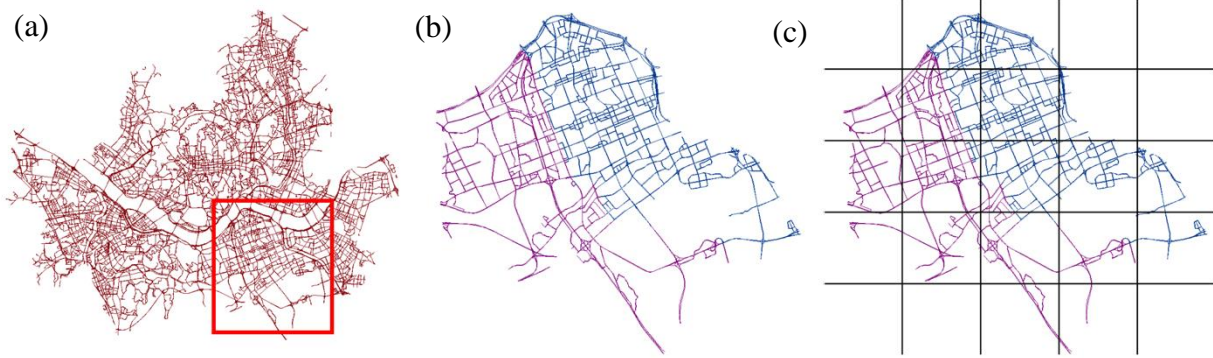


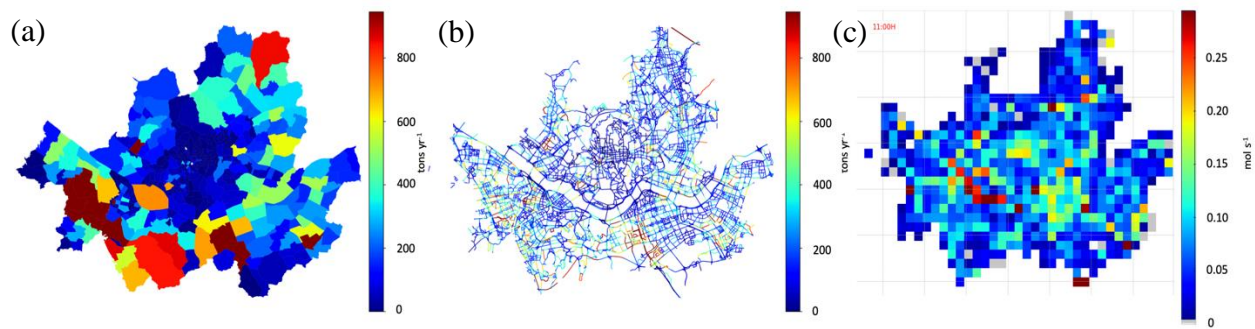
**Figure 5.** The schematic of modules and their functions in the CARS.



1032  
1033  
1034  
1035

**Figure 6** (a) the road network GIS shapefile of Seoul, South Korea; (b) two districts with different colors (purple and blue); (c) the modeling grid cells over road segments.

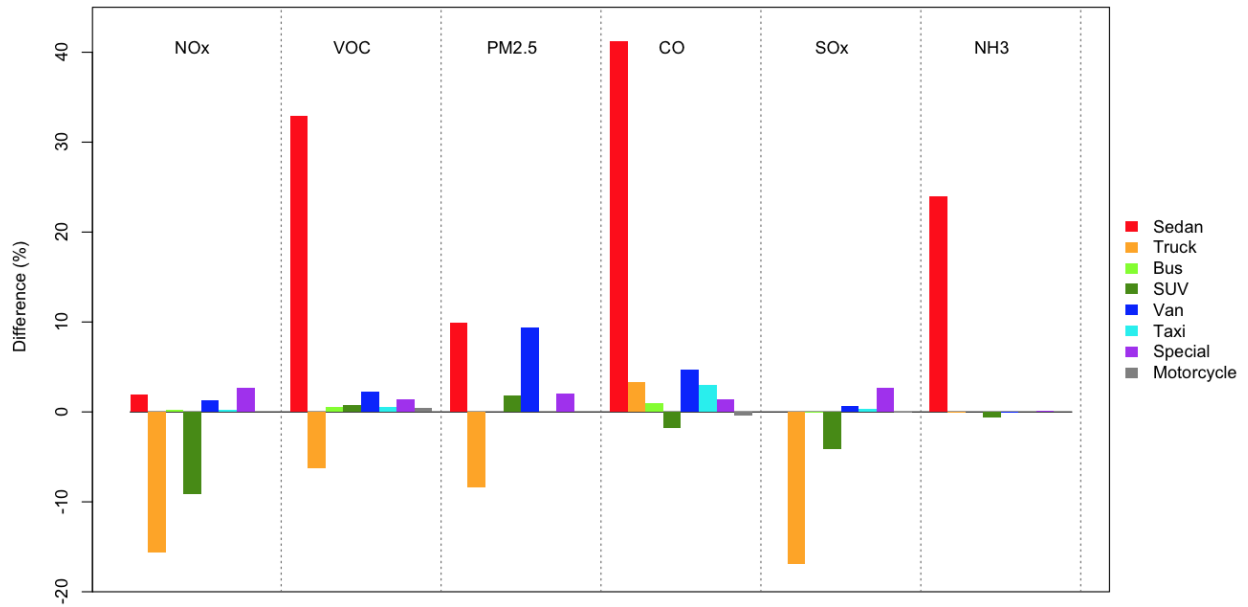




1036

1037 **Figure 7.** Three different formats of CO emissions from CARS, (A) District-level total emissions  
 1038 ( $\text{t yr}^{-1}$ ) (B) Link-level total emissions ( $\text{t yr}^{-1}$ ), (C) CTM-ready gridded hourly total emissions (moles  
 1039  $\text{s}^{-1}$ ).

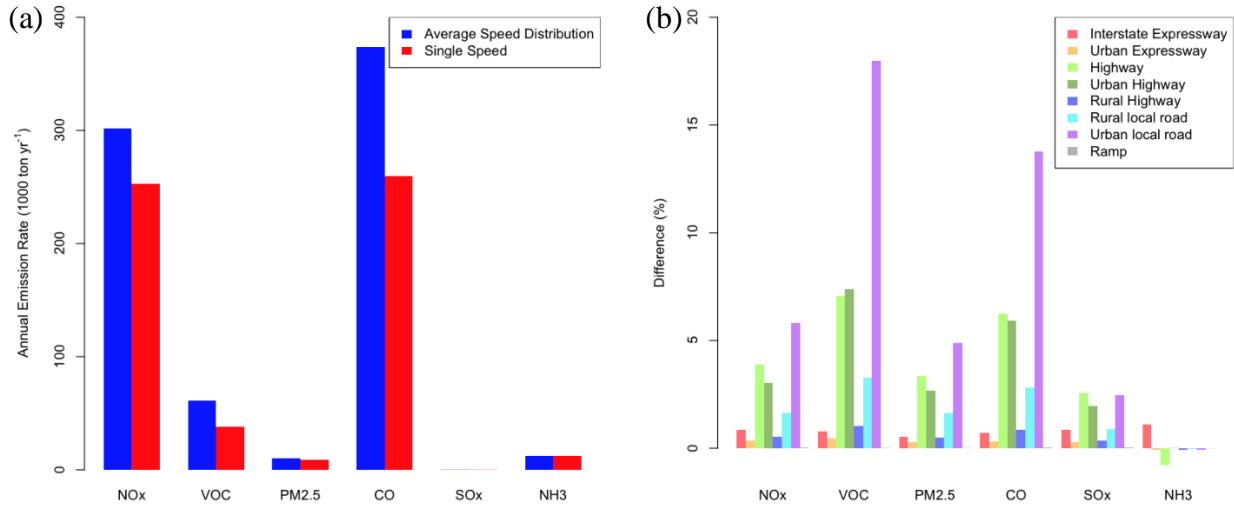
1040



1041  
 1042  
 1043  
 1044

**Figure 8.** Comparison between CARS 2015 and CAPSS 2015 onroad mobile emissions inventories by vehicle types. The standard line is CAPSS 2015 data.

1045



1046  
1047  
1048  
1049

**Figure 9.** The impacts of emissions between the ASD and single-speed approach: (a) the total emission differences by pollutant; (b) The road-specific difference (%) by pollutant.

1050 **Appendices**

1051

1052

1053 **Appendix A:** The vehicle types classified by fuel type, vehicle body type, and engine size. The  
 1054 emission factors of the diesel vehicle with the star (\*) are depended on the ambient temperature  
 1055 (*T*).

Vehicle Types	Fuel Types							
	Gasoline	Diesel	LPG	CNG	HYBRID_G	HYBRID_D	HYBRID_L	HYBRID_C
Sedan	Supercompact	Supercompact*	Supercompact	-	-	-	-	-
	Compact	compact*	compact	compact	compact	compact	compact	-
	Fullsize	Fullsize*	Fullsize	Fullsize	Fullsize	Fullsize	Fullsize	-
	Midsize	Midsize*	Midsize	Midsize	Midsize	Midsize	Midsize	-
Truck	Supercompact	Supercompact	Supercompact	-	-	-	-	-
	Compact	Compact*	Compact	Compact	-	-	-	-
	Fullsize	Concrete	-	Fullsize	-	-	-	-
	Midsize	Fullsize	Midsize	Midsize	-	-	-	-
	-	Midsize	-	-	-	-	-	-
	-	Dump	-	-	-	-	-	-
	-	Special	Special	Special	-	-	-	-
Bus	Urban	Urban	Urban	Urban	-	Urban	-	-
	-	Rural	-	Rural	-	Rural	-	Rural
SUV	Compact	Compact*	Compact	-	-	-	-	-
	Midsize	Midsize*	Midsize	Midsize	Midsize	-	-	-
Van	supercompact	supercompact	supercompact	-	-	-	-	-
	Compact	Compact	Compact	Compact	-	-	-	-
	-	-	Fullsize	Fullsize	Fullsize	Fullsize	Fullsize	Fullsize
	Midsize	Midsize	Midsize	Midsize	Midsize	Midsize	Midsize	Midsize
Taxi	-	-	Compact	-	-	-	-	-
	-	-	Fullsize	-	-	-	-	-
	-	-	Midsize	-	-	-	-	-
Special	-	Tow	-	-	-	-	-	-
	Wrecking	Wrecking	Wrecking	Wrecking	-	-	-	-
	Others	Others	Others	-	-	-	-	-
Motorcycle	Compact	-	-	-	-	-	-	-
	Midsize	-	-	-	-	-	-	-
	Fullsize	-	-	-	-	-	-	-

1056 - no existence

1057 \* ambient temperature-dependent diesel vehicle

1058 LPG: Liquefied Petroleum Gas

1059 CNG: Connecticut Natural Gas

1060 Hybrid\_G: hybrid vehicle with gasoline

1061 Hybrid\_D: hybrid vehicle with diesel

1062 Hybrid\_L: hybrid vehicle with LPG

1063 Hybrid\_C: hybrid vehicle with CNG

1064

1065

1066 **Appendix B**, The summary of activity data (number of vehicles and daily total VKTs) in South  
 1067 Korea by vehicle type with engine size.

Vehicle Types	Engine sizes	Fuel Types									
		Gasoline		Diesel		LPG		CNG		Hybrid	
		Numbers	Daily VKT	Numbers	Daily VKT	Numbers	Daily VKT	Numbers	Daily VKT	Numbers	Daily VKT
Sedan	Supercompact	1,792,471	50,197,345	46	1,761	83,226	4,000,067	6	237	-	-
	Compact	1,372,317	39,543,668	51,324	2,570,086	8,040	257,060	276	12,115	3,802	137,360
	Fullsize	2,403,327	100,632,702	428,831	20,928,552	292,850	15,910,588	5,296	323,852	21,533	1,086,509
	Midsized	4,858,533	167,454,032	672,960	33,126,318	1,431,970	66,640,378	4,310	625,717	140,527	6,717,856
Truck	Supercompact	850	9,595	816	354	111,051	6,550,476	-	-	-	-
	Compact	3,185	143,510	2,655,089	133,480,216	87,650	3,567,109	42	2,694	-	-
	Fullsize	3	422	180,991	25,774,819	-	-	72	4,676	-	-
	Midsized	98	7,430	258,509	17,477,685	1,434	47,870	14	483	-	-
	Dump	-	-	-	-	-	-	-	-	-	-
	Special	20	970	-	-	2,292	99,124	1,194	60,886	-	-
Bus	Urban	1	126	40,448	7,282,593	1	652	6,543	1,466,854	2	282
	Rural	-	-	34,997	6,334,278	-	-	30,792	6,460,001	216	50,873
SUV	Compact	42,348	1,395,153	2,341,397	105,962,626	6,946	275,728	13	551	-	-
	Midsized	91,002	3,520,552	1,120,128	5,277,861	13,567	595,426	15	706	1,719	88,683
Van	supercompact	88	1,645	-	-	44,947	2,058,014	-	-	-	-
	Compact	2,937	87,507	685,317	34,781,937	151,654	6,135,138	7	255	-	-
	Fullsize	-	-	19,452	1,318,221	1	14	97	7,598	3	136
	Midsized	2	1,303,795	31,790	1,433,407	15	416	160	15,216	2	85
	Special	-	-	-	-	-	-	-	-	-	-
Taxi	Compact	-	-	-	-	8,380	576,378	-	-	-	-
	Fullsize	-	-	-	-	92,861	10,827,756	-	-	-	-
	Midsized	-	-	-	-	474,455	69,087,721	-	-	-	-
Special	Tow	-	-	40,807	7,447,773	-	-	-	-	-	-
	Wrecking	2	138	12,568	813,746	128	6,607	3	94	-	-
	Others	47	553	28,275	989,988	180	9,966	-	-	-	-
Motorcycle	Compact	184,822	3,507,948	-	-	-	-	-	-	-	-
	Fullsize	65,964	3,493,728	-	-	-	-	-	-	-	-
	Midsized	1,910,988	61,676,824	-	-	-	-	-	-	-	-

- 1068 - no existence
- 1069 LPG: Liquefied Petroleum Gas
- 1070 CNG: Connecticut Natural Gas
- 1071 Hybrid: all hybrid vehicles, electric power mixed with fossil fuel (gasoline, diesel, LPG, or CNG)
- 1072
- 1073
- 1074

1075  
1076

**Appendix C**, Eight road types with assigned average vehicle operating speed and VKT fractions.

Road types	Description	Average Speed (km h <sup>-1</sup> )	Road VKT fraction
101	Interstate Expressway	90	41%
102	Urban Expressway	60	5%
103	Highway	58	18%
104	Urban Highway	36	12%
105	Rural Highway	55	3%
106	Rural Local Road	45	4%
107	Urban Local Road	32	17%
108	Ramp	50	0.4%

1077  
1078

1079 **Appendix D**, The daily average VKT (km d<sup>-1</sup>) per vehicle by vehicle and fuel types.

Vehicle types	Fuel Types					
	Gasoline	Diesel	LPG	CNG	Hybrid	Average
Sedan	34	49	48	97	48	38
Truck	39	57	51	52	-	57
Bus	126	180	-	212	237	191
SUV	37	46	42	45	52	46
VAN	29	51	42	87	44	49
Taxi	-	-	140	-	-	140
Special	14	113	54	31	-	113
Motorcycle	32	-	-	-	-	32

1080  
1081

1082 **Appendix E**, Average speed distribution (ASD) for each road type: The table columns are  
 1083 different road types, and the table rows are average speed of each speed bin.

Speed bins	Speed (km/h)	Road Types							
		101	102	103	104	105	106	107	108
1	speed < 4	1.50%	2.00%	5.00%	5.00%	5.00%	10.00%	10.00%	0.00%
2	4 ≤ speed < 8	0.50%	1.00%	2.00%	2.00%	2.00%	5.00%	5.00%	0.00%
3	8 ≤ speed < 16	0.00%	0.33%	0.40%	3.59%	0.41%	0.30%	2.76%	0.11%
4	16 ≤ speed < 24	0.00%	1.09%	3.64%	14.35%	1.45%	2.91%	11.75%	5.85%
5	24 ≤ speed < 32	0.01%	3.04%	6.82%	35.25%	6.85%	6.15%	40.80%	12.80%
6	32 ≤ speed < 40	0.17%	6.43%	9.28%	17.14%	14.70%	12.00%	12.69%	24.53%
7	40 ≤ speed < 48	0.52%	14.76%	10.70%	10.86%	16.20%	23.30%	7.49%	23.74%
8	48 ≤ speed < 56	0.53%	16.66%	12.52%	5.72%	15.42%	20.72%	4.24%	6.60%
9	56 ≤ speed < 64	1.94%	23.49%	12.83%	2.68%	6.08%	10.06%	2.56%	10.90%
10	64 ≤ speed < 72	5.05%	16.30%	10.51%	1.90%	13.21%	3.84%	1.45%	5.30%
11	72 ≤ speed < 80	11.70%	10.19%	12.69%	0.74%	9.98%	2.85%	0.53%	5.30%
12	80 ≤ speed < 89	28.73%	4.30%	12.21%	1.04%	6.75%	2.21%	0.65%	4.59%
13	89 ≤ speed < 97	34.24%	0.51%	1.82%	0.15%	1.90%	0.62%	0.08%	0.00%
14	97 ≤ speed < 105	14.99%	0.00%	0.02%	0.00%	0.04%	0.03%	0.00%	0.30%
15	105 ≤ speed < 113	0.18%	0.00%	0.00%	0.00%	0.00%	0.00%	0.00%	0.00%
16	113 ≤ speed < 121	0.01%	0.00%	0.00%	0.00%	0.00%	0.00%	0.00%	0.00%

1084 **Appendix F**: Single average speed for each road type

Speed bins	Speed (km/h)	Road Types							
		101	102	103	104	105	106	107	108
1	speed < 4	0%	0%	0%	0%	0%	0%	0%	0%
2	4 ≤ speed < 8	0%	0%	0%	0%	0%	0%	0%	0%
3	8 ≤ speed < 16	0%	0%	0%	0%	0%	0%	0%	0%
4	16 ≤ speed < 24	0%	0%	0%	0%	0%	0%	0%	0%
5	24 ≤ speed < 32	0%	0%	0%	0%	0%	0%	100%	0%
6	32 ≤ speed < 40	0%	0%	0%	100%	0%	0%	0%	0%
7	40 ≤ speed < 48	0%	0%	0%	0%	0%	100%	0%	100%
8	48 ≤ speed < 56	0%	0%	100%	0%	100%	0%	0%	0%
9	56 ≤ speed < 64	0%	100%	0%	0%	0%	0%	0%	0%
10	64 ≤ speed < 72	0%	0%	0%	0%	0%	0%	0%	0%
11	72 ≤ speed < 80	0%	0%	0%	0%	0%	0%	0%	0%
12	80 ≤ speed < 89	100%	0%	0%	0%	0%	0%	0%	0%
13	89 ≤ speed < 97	0%	0%	0%	0%	0%	0%	0%	0%
14	97 ≤ speed < 105	0%	0%	0%	0%	0%	0%	0%	0%
15	105 ≤ speed < 113	0%	0%	0%	0%	0%	0%	0%	0%
16	113 ≤ speed < 121	0%	0%	0%	0%	0%	0%	0%	0%

1085

1086 **Appendix G:**

1087  
 1088 The annual emission rate between original road type ASD, adjusted road type ASD, and CAPSS  
 1089 result for 2015

Gg/year	CO	NOx	SOx	PM10	PM2.5	VOC	NH3
CARS data 2015 org ASD	269.3	258.4	0.2	9.5	8.8	38.9	12.4
CARS data 2015 adj ASD	373.9	301.8	0.2	11.0	10.1	61.2	12.5
CAPSS 2015	245.5	369.6	0.2	9.6	8.8	46.1	10.1

1090  
 1091  
 1092  
 1093 **Appendix H:**

1094 CARS model input data summary table

Input data type	Parameters	Variable Name in CARS	File format
<b>Human activity data of each vehicle</b>	Fuel, vehicle, type, daily VKT, region code, manufacture data	activity_file	csv
<b>Emission factor table</b>	Vehicle, engine, fuel, SCC ,Pollutant, year, temperature, v,a,b,c,d,f,k	Emis_factor_list	csv
<b>Link level Shape file</b>	Link ID, region code, region name, road rank, speed, VKT, Link length, geometry	Link_shape	shape file
<b>County Shape File</b>	Region code, region name	county_shape	shape file
<b>Average speed distribution table</b>	Speed bins, the distribution of each road type	avg_SPD_Dist_file	csv
<b>road restriction table</b>	Vehicle, engine, fuel, road types	road_restriction	csv
<b>Vehicle deterioration table</b>	Vehicle, engine, SCC, fuel, Pollutant, Manufacture date	Deterioration_list	csv
<b>Control strategy factors table</b>	Vehicle, engine, fuel, year, data, region code, control factor	control_list	csv
<b>Model domain description</b>	Projection method name, parameters for prjection method, domain name, bottum left coner X and Y, grid cell size, numbers of grid cell in X, Y, and Z-axis	gridfile_name	text file in griddesc format
<b>Temporal profile tables</b>	Profile reference number, Year to Monthly profile (12 columns)	temporal _monthly_file	csv
	Profile reference number, week to daily profile (7 columns)	temporal _week_file	csv



	Profile reference number, week day to hourly profile (24 columns)	temporal_weekday_file	csv
	Profile reference number, weekend day to hourly profile (24 columns)	temporal_weekend_file	csv
	Vehicle, types, fuel, road type, month reference number, week reference number, weekday reference number, weekend reference number	temporal_CrossRef	csv
<b>Chemical profile table</b>	Species code, species name, target species name, fraction, molecular weight,	Chemical_profile	txt or csv
	Vehicle, engine, fuel, species reference codes	speciation_CrossRef	csv

1096  
1097